Robust Integration of Electric Vehicles Charging Load in Smart Grid's Capacity Expansion Planning

Sajad Aliakbari Sani *[1], Olivier Bahn[1], Erick Delage[1], and Rinel Foguen Tchuendom[2]

[1]GERAD and Department of Decision Sciences, HEC Montréal, Montréal, Canada, H3T 2A7.
[2]GERAD, CIM and McGill University, Montréal, Canada, H3A 0C3.

July 22, 2021

Abstract

Battery charging of electric vehicles (EVs) needs to be properly coordinated by electricity producers to maintain the network reliability. In this paper, we propose a robust approach to model the interaction between a large fleet of EV users and utilities in a long-term generation expansion planning problem. In doing so, we employ a robust multi-period adjustable generation expansion planning problem, called R-ETEM, in which demand responses of EV users are uncertain. Then, we employ a linear quadratic game to simulate the average charging behavior of the EV users. The two models are coupled through a dynamic price signal broadcasted by the utility. Mean field game theory is used to solve the linear quadratic game model. Finally, we develop a new coupling algorithm between R-ETEM and the linear quadratic game with the purpose of adjusting in R-ETEM the uncertainty level of EV demand responses. The performance of our approach is evaluated on a realistic case study that represents the energy system of the Swiss "Arc Lémanique" region. Results show that a robust behaviorally-consistent generation expansion plan can potentially reduce the total actual cost of the system by 6.2% compared to a behaviorally-inconsistent expansion plan.

Keywords : Multi-period adjustable robust optimization, Mean field game, Demand response, Electric vehicles.

1 Introduction

Modeling the interaction between electric vehicles (EVs) and utilities (electricity producers) is an important problem in smart grid (SG) management because utilities need to properly coordinate the EVs load. On the one hand, EVs are a mobile load that is highly spatial and temporally uncertain, on the other hand, due to their vehicle-to-grid (V2G) features, EVs can provide the network with ancillary services and distributed storage if they are properly coordinated. In other words, utilities need to

*corresponding author
Email addresses: *sajad.aliakbarisani@hec.ca*, *olivier.bahn@hec.ca*, *erick.delage@hec.ca*, *rinel.foguen@gerad.ca*

partially control the EV load profile to prevent network congestions and load imbalances. In addition, since EVs run on battery, utilities can take advantage of this distributed storage in order to increase the reliability of the network by valley-filling and peak-shaving of the power consumption profile. Usually, utilities use incentive pricing as a leverage to coordinate EV load in so-called demand response (DR) programs. Nevertheless, the operational planning is still challenging because the response of EV users to the price signals is uncertain. This uncertainty becomes even more important in a generation expansion planning (GEP) problem, where the planner needs to estimate the reserved capacity provided by DR programs over a long-term horizon. Let us recall here that GEP is the problem of determining the required capacity of a power network to satisfy demand at minimum cost, while also satisfying economic, environmental and technical constraints (see for a recent review Koltsaklis and Dagoumas 2018).

Game theory and bi-level optimization are the main mathematical tools used to model the interaction between EV users, or consumers/prosumers in a broader perspective, and the electricity network (for example, see Mohsenian-Rad et al. 2010, Zugno et al. 2013, Wang et al. 2019, Zeng et al. 2020). In this literature, EV users play a non-cooperative game to decide on i) when and how much to consume electricity to charge the battery, and ii) when and how much to provide service to the network. Their behavior is impacted by the electricity price broadcasted by a utility or a local DR aggregator. Whereas the utility solves its own problem to maximize its profit from generating electricity or buying it from a wholesale market. This implies that the utility needs to design a dynamic price signal to induce consumers/prosumers to behave in such a way that their aggregated behavior maximizes its profit. To solve these models, a complementarity problem or Karush–Kuhn–Tucker conditions are usually used to reformulate the original problem into a mixed integer linear programming (MILP) problem, which is solved using column and constraint generation techniques. This approach works well when the number of players is small. From an application point of view, these problems model a short-term interaction between a local utility and a limited number of EVs connected to its network. But when the number of players increases, finding some equilibrium becomes computationally challenging. For example, to model the effect of EV interactions on the strategic long-term GEP problem, one needs to model the behavior of a fleet of EVs with a very large number of players connected to the whole network. To circumvent this issue, the theory of mean field games (MFG), introduced simultaneously by Huang et al. (2006) and Lasry and Lions (2006), provides a methodology to obtain some ϵ-Nash equilibrium, with vanishing errors as the pool size goes to infinity.

While there are many papers that address the interaction between a local utility and a small group of EVs over a short-term horizon, there is only a limited number of papers that address the influence of charging behavior of a large fleet of EVs on a long-term GEP problem (see Babonneau et al. 2016, 2020, as two examples). Babonneau et al. (2016) model the influence of the aggregated EV charging on GEP using a large-scale LP problem. In order to to do so, it is necessary to assume that i) all EVs share the same constraints concerning their utilization, ii) EV users are only seeking to minimize their cost, and iii) the latter is a convex function with respect to the total load. Moreover, the analysis in Babonneau et al. (2016) is limited to a deterministic setting. In a more realistic formulation of the interaction between a large population of EVs connected to a distribution network and a GEP problem, Babonneau et al. (2020) couple a long-term GEP problem, called ETEM, with a Wardrop equilibrium-based model. Moreover, in order to analyze the interaction in a stochastic setting, they develop a MFG model of battery charging and couple it with a robust version of ETEM.

In this paper, we propose a new scheme for robustly integrating the average collective charging behavior of a fleet of EVs in a long-term GEP problem. Specifically, we use the approach in Aliakbarisani et al. (2020) to robustify a specific GEP problem, called ETEM, against the perturbations of the demand response of a fleet of EVs connected to the network. The proposed robust ETEM

(R-ETEM) is a multi-stage robust optimization problem, where in a first stage one decides on the capacity expansion and planned demand response, then after observing the actual demand response one can decide on the optimal procurement of energy in each period. To model the EV users' behavior, we employ the linear quadratic game (LQG) presented in Tchuendom et al. (2019). This LQG is a finite horizon game among a large number of EV users, who selfishly optimize a cost function that accounts for their daily usage, desired level of charge of the EV battery, its degradation due fast charging, and regional dynamic electricity prices that correspond to the marginal costs of electricity in R-ETEM. MFG theory is used to formulate and solve the LQG.

The main contribution of this paper consists in developing a new coupling algorithm between a long-term risk averse expansion planning model (R-ETEM) and a short-term higher-precision consumer behavior model (LQG). The aim of this coupling is to identify a robust optimal capacity expansion plan that is immunized against the demand response deviations observed in the behavioral model when it is implemented. Such optimal robust plans will be referred to as being behaviorally-consistent and will be optimized using a bisection method that converges in $O(\log(1/\varepsilon))$ iterations. We further provide a numerical illustration that highlights the impact of our approach on the expansion planning of electricity generation capacities in the real context of the Arc Lémanique region (in Switzerland), where our robust strategy significantly reduces the realized total cost.

The remainder of the paper is organized as follows. In Section 2, we present an overview of different methods to model the interaction between consumers, prosumers (and EV users in particular), and utilities. Moreover, we position our work with respect to closely related studies that address uncertainty in a GEP problem, with a special focus on ETEM. In Section 3, we present the formulation of R-ETEM. Section 4 formulates the LQG and describes how MFG theory is used to identify an ϵ-Nash equilibrium. Section 5 presents the new coupling algorithm that identifies behaviorally-consistent robust capacity expansion plans. Section 6 presents and discusses numerical results for our case study. Finally, Section 7 provides concluding remarks.

2 Literature review

In this section we briefly review the methods that are used in the literature to formulate the interaction between EV users, or other consumers/prosumers, and the electricity network. Then, we summarize some closely related studies that address uncertainties in a GEP problem.

Modeling the interaction between EV users and the electricy network has been addressed in many studies. Zeng et al. (2020) develop a bi-level robust optimization to model the effect of charging behavior of a number of EVs on the configuration of a charging station. The charging station is connected to the network and dynamically decides on the amount of energy to be purchased from, and injected to the network. They apply a complementarity theory to reformulate the so-called adversarial problem into a MILP and use a column-and-constraint generation algorithm to solve it. Zugno et al. (2013) propose a bi-level optimization model to formulate the interaction between the energy retailer and a number of partially flexible consumers. The retailer faces uncertainties in market price and in demand (due to weather conditions). They reformulate the problem to be cast as a single-level MILP problem. Wang et al. (2019) develop a stackelberg game between an electricity aggregator and EV users. The upper level optimization problem maximizes the profit of the aggregator who purchases electricity from the wholesale market and signals a dynamic price to a group of EV users. The lower level problem, on the other hand, minimizes the charging cost of each EV. They use an iterative algorithm to solve the problem. Mohsenian-Rad et al. (2010) propose a game theoretic approach for modeling the interaction between N prosumers who want to schedule a set of flexible loads in response to the dynamic tariffs which are broadcasted by the utility. They show that under some

assumptions, including that the prosumers would be only cost minimizer and their total cost function would be convex, a unique Nash equilibrium can be obtained from solving a MILP problem. They propose a distributed algorithm as well in order to find the Nash equilibrium and solve an example with N=20 players. As discussed before, these papers use a game theoretic approach to formulate the interactions. They then use complementarity condition to turn the problem into a single optimization problem. From a computational point of view, this type of approach works well with a limited number of players. However, when the number of players increases, other methodologies, like MFG, become more appropriate (see, for example, Couillet et al. 2012, Ma et al. 2013, Chen et al. 2014, Zhu et al. 2016, Lindholm et al. 2017, Gomes and Saude 2018, Tchuendom et al. 2019).

Generation expansion planning (GEP) is a classical power system problem that plans the capacity expansion strategy of the entire electricity network over a long-term horizon to satisfy demand at minimum cost (see Koltsaklis and Dagoumas (2018) for a recent review). With the advent of smart grids, recent versions of the GEP problem consider DR as a reserved capacity (see e.g. Babonneau et al. 2017, Lohmann and Rebennack 2017). Because of the long-term horizon of the planning in a GEP, this problem is plagued with many uncertainties. To tackle this issue, multi-stage versions of Robust Optimization (RO) and Stochastic Programming (SP) have been widely used (Dehghan et al. 2014, Mejía-Giraldo and McCalley 2014, Han et al. 2018, Zou et al. 2018, Aliakbarisani et al. 2020). Specifically, Bloom (1983) and Bloom et al. (1984) are among the first papers to propose a two-stage SP formulation for the GEP problem with uncertain demand and supply. In Dehghan et al. (2014), the uncertainties of demand and investment cost are modeled in a two-stage RO model, while Mejía-Giraldo and McCalley (2014) uses such a formulation to address uncertainty in fuel price, demand and transmission capacity. Han et al. (2018) model the uncertainty of load demand and wind output in a GEP using a two-stage SP. Zou et al. (2018) propose a partially adaptive multi-stage SP GEP problem, where fuel price and demand are the two sources of uncertain.

Recently, Aliakbarisani et al. (2020) developed a robust multi-period conservative approximation formulation to address the uncertainty of DR in the ETEM model. This is the formulation that will be used in this paper for handling demand response uncertainty caused by a large fleet of EV users. Unlike Aliakbarisani et al. (2020), who simply assumed that DR deviations were exogenous to the expansion plan and thus that the size of the uncertainty set could be calibrated using historical data, our proposed approach will consider DR deviations to be endogenous, i.e. that they are affected by the marginal cost of useful energy production under the optimized expansion plan. Such endogeneity will be modeled using a continuous time linear quadratic game played by the EV users. The novelty in our approach consists in designing a procedure that will ensure that the robust expansion plan is both minimal with respect to worst-case cost and immunized against EV users' behavior as they react to the resulting marginal cost of energy.

Our work is similar in spirit to Babonneau et al. (2020), who were the first to attempt to integrate EV charging behavior in a robust version of ETEM. There are however crucial distinctions between the two works. First, the robust expansion planning model in Babonneau et al. (2020) only considers "here and now" decisions (a.k.a. static policies) and accounts for uncertainty about the maximum and minimum value that the demand response decision can take. They also take an optimistic view on robustness by robustifying only the sum of demand responses over the horizon instead of on a period by period basis. Secondly, the nature of the solution that they obtain when reaching a solution at equilibrium between the R-ETEM formulation and the LQGs is very different. To the best of our knowledge, their "robust" solution is only guaranteed to prescribe a **plausible** demand response plan, i.e. within the range of the more likely demand response profiles produced by the LQGs under market clearing prices. Such a solution actually has no guarantees regarding worst-case cost when the actual demand response deviates from the optimally selected plausible one. In opposition, our solution will

provide (and minimize) a guarantee on the worst-case cost achieved by the expansion plan under all demand response deviation profiles produced by the LQGs under market clearing prices. We refer interested readers to Appendix B for more details about these distinctions. Finally, unlike Babonneau et al. (2020), which only present a simple step by step illustration of their algorithm, we perform a more detailed numerical investigation of how our new robust modeling approach affects the expansion planning of the electricity network of the Arc Lémanique region.

3 A robust multi-period ETEM model

In this work we consider the ETEM model proposed in Babonneau et al. (2017) (and summarized in Appendix A). ETEM is a multi-regional multi commodity GEP problem. Its description is based on a list of geographical regions indexed by $l \in \mathbb{L}$, a list of energy commodities $c \in \mathbb{C}$, and a list of technologies $p \in \mathbb{P}$. The planning horizon, which typically spans over 40 years or more, is divided into different decision making periods, denoted as $t \in \mathbb{T}$, that are themselves divided into several time-slices in each period that capture the pattern of consumption i.e., $s \in \mathbb{S} := \mathbb{H} \times \mathbb{J}$ based on the hour of the day $h \in \mathbb{H}$ and season of the year $j \in \mathbb{J}$. ETEM is able to model both consumers and prosumers on the demand side, but in this paper we focus on consumers. For example, our implementation will consider a $T = 8$ decision making periods each representing 5 years, while the time-slices will model the differences in consumption at a seasonal level ($\mathbb{J} := \{$winter, summer, intermediate seasons$\}$) and hourly level (with 4 different hour blocks as shown in Table 1). In total, there are 12 time-slices in a year $|\mathbb{S}| = 12$ (see Figure 1). Decisions in ETEM include (i) annual installation of each technology in each region, (ii) energy production by each technology in each region and each period and time slice, (iii) import of energy commodity from outside of the energy system, (iv) export of energy to outside of the energy system, (v) transmission of energy from one region to another region inside the boundary of the energy system, and finally (vi) planned demand response for the useful demand. In this paper, in order to simplify the presentation, we use a similar vector representation as used in Aliakbarisani et al. (2020), where $\boldsymbol{x} \in \mathbb{R}^m$ captures the technology installation decisions (i) in all periods and all regions while $\boldsymbol{y}_i$ captures the procurement decisions (ii-v) of all commodities, in all regions and time slices that belong to season $i \in \mathbb{I} := \mathbb{T} \times \mathbb{J}$, the set of seasonal periods. We depart from the notation in Aliakbarisani et al. (2020) by using a dedicated $\boldsymbol{s}_i$ to relate to demand response decisions in order to permit us to define the interaction with the consumption behavior model. Overall, the deterministic version of ETEM takes the form:

$$\min_{\boldsymbol{x}, \{\boldsymbol{y}_i, \boldsymbol{s}_i\}_{i=1}^{|\mathbb{I}|}} \quad f^\top \boldsymbol{x} + \sum_{i \in \mathbb{I}} h_i^\top \boldsymbol{y}_i \tag{1a}$$

$$\text{s.t.} \quad A_i \boldsymbol{x} + E_i \boldsymbol{s}_i + B_i \boldsymbol{y}_i \leq b_i, \ \forall i \in \mathbb{I} \tag{1b}$$

$$F_i \boldsymbol{s}_i \leq U_i, \ \boldsymbol{s}_i \geq 0 \quad \forall i \in \mathbb{I} \tag{1c}$$

$$D\boldsymbol{x} \leq e\,, \tag{1d}$$

where constraint (1b) represents the set of constraints on capacity, seasonal procurement and useful demand. For example, these constraints include, but are not limited to, energy balance, minimum required reserve capacity for peak periods, demand, and capacity factor constraints (see Appendix A). On the other hand, constraint (1c) limits the feasible space for demand response and constraint (1d) imposes technical and economical constraints on the newly installed capacity. More importantly for what will follow, in terms of demand response modeling, constraint (1b) includes:

$$\sum_{p \in \mathbb{P}_c^P} \boldsymbol{P}_{t,s,l,p,c} \geq \Theta_{t,l,c} \boldsymbol{V}_{t,s,l,c} \qquad \forall t, s, l, c \in \mathbb{C}^{\mathcal{D}} \tag{2}$$

Table 1: Definition of hourly blocks $\mathbb{H}$

h_1	23 pm - 6 am
h_2	6 am - 12 pm
h_3	12 pm - 17 pm
h_4	17 pm- 23 pm

while (1c) contains:

$$\upsilon_{t,s,l,c}(1-\nu_{t,s,l,c}) \leq \boldsymbol{V}_{t,s,l,c} \leq \upsilon_{t,s,l,c}(1+\nu_{t,s,l,c}) \quad \forall t,s,l,c \in \mathbb{C}^{\mathcal{D}} \tag{3}$$

$$\sum_{s\in\mathcal{S}_j} \boldsymbol{V}_{t,s,l,c} = \sum_{s\in\mathcal{S}_j} \upsilon_{t,s,l,c} \qquad \forall t,l,c \in \mathbb{C}^{\mathcal{D}}, j \in \mathbb{J} \tag{4}$$

Together, these constraints model the idea that for each commodity c in the set of useful demand $\mathbb{C}^{\mathcal{D}}$, the total production of useful energy accounted for by $\boldsymbol{P}$ must satisfy the demand in each time-slice and region. The latter demand is a result of relative demand response plan denoted by $\boldsymbol{V}$ that attempts to optimally distribute the total demand of period t into all time-slices s inside period t, while staying within a certain ν margin from the nominal demand distribution v. Finally, note that $\boldsymbol{s}_i$ captures all $\boldsymbol{V}_{t,s,l,c}$ with $i=(t,j)$, $l \in \mathbb{L}$, $s \in \mathbb{S}_j$, and all $c \in \mathbb{C}^{\mathcal{D}}$.

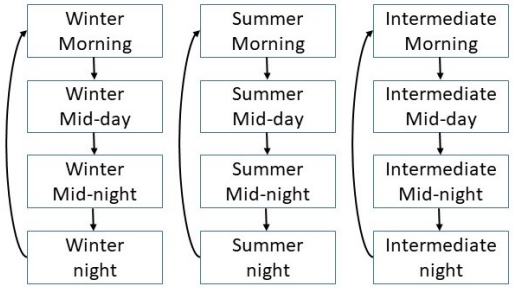

Figure 1: Sequence of time-slices

As described previously, beside the optimal expansion of the generation technologies, the planner decides in ETEM of the optimal level of DR contributions. It is therefore assumed that the consumers can be convinced to behave according to the planned demand response by using incentive programs such as real-time pricing. While, in long-term planning problem such as GEPs, there are necessarily many uncertainties that may affect the performance of the expansion plans, in this paper we focus on the influence of consumer behavioral uncertainties on the performance that can be expected from planned demand response. In particular, we assume that the planner wishes to immunize his expansion plan against possible deviations between the planned and actual DR. As shown in Aliakbarisani et al. (2020), this can be done by employing a R-ETEM model, which offers a protection against relative demand response deviations (RDRDs) in ETEM.

Mathematically speaking, R-ETEM considers that the total demand of final energy is perturbed by a relative demand response deviation (RDRD) denoted by $\boldsymbol{\delta}_{t,s,l,c}$, i.e that $\Theta_{t,l,c}\boldsymbol{V}_{t,s,l,c}$ in constraint (2) is replaced with $\Theta_{t,l,c}\big(\boldsymbol{V}_{t,s,l,c}+\boldsymbol{\delta}_{t,s,l,c}\big)$ with $\boldsymbol{\delta}$ in some uncertainty set $\Xi(\eta)$ defined as:

$$\Xi(\eta) = \left\{ \boldsymbol{\delta} \in \mathbb{R}^d \;\middle|\; \begin{array}{c} \exists \boldsymbol{\zeta} \in [-1,\,1]^d \\ \boldsymbol{\delta}_{t,s,l,c} = \eta \boldsymbol{\zeta}_{t,s,l,c},\ \forall t,s,l,c \in \mathbb{C}^U \\ \sum_{s\in\mathbb{S}^j}\sum_{l\in\mathbb{L}}\sum_{c\in\mathbb{C}^U} |\boldsymbol{\zeta}_{t,s,l,c}| \leq \sqrt{|\mathbb{S}^j||\mathbb{C}^U||\mathbb{L}|}\ \forall t,j \in \mathbb{J} \end{array} \right\}, \tag{5}$$

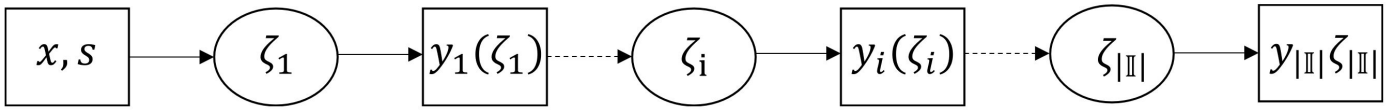

Figure 2: Sequence of decisions and uncertainty observations in our multi-period problem

where d is the total number of perturbations while η captures the level of uncertainty in Ξ and can be used to model the level of robustness (or conservatism) of the R-ETEM formulation. Note that unlike the budgeted uncertainty set used in Aliakbarisani et al. (2020), our choice of Ξ encodes the Cartesian product of polyhedral outer approximations of norm-2 balls of radius η, in order to avoid making the assumption that $\boldsymbol{\delta}$ has a known bounded support. Furthermore, based on constraints (3) and (4), one can establish the largest possible amount of deviation implied by the ETEM model to be:

$$\bar{\eta} := \max_{\boldsymbol{\delta}} \quad \min_{\eta:\boldsymbol{\delta}\in\Xi(\eta)} \eta \tag{6a}$$

$$\text{s.t.} \quad \boldsymbol{V}_{t,s,l,c} + \boldsymbol{\delta}_{t,s,l,c} \geq \upsilon_{t,s,l,c}(1-\nu_{t,s,l,c}) \quad \forall t,s,l,c \in \mathbb{C}^{\mathcal{D}} \tag{6b}$$

$$\boldsymbol{V}_{t,s,l,c} + \boldsymbol{\delta}_{t,s,l,c} \leq \upsilon_{t,s,l,c}(1+\nu_{t,s,l,c}) \quad \forall t,s,l,c \in \mathbb{C}^{\mathcal{D}} \tag{6c}$$

$$\sum_{s\in\mathcal{S}_j} \boldsymbol{V}_{t,s,l,c} + \boldsymbol{\delta}_{t,s,l,c} = \sum_{s\in\mathcal{S}_j} \upsilon_{t,s,l,c} \qquad \forall t,l,c \in \mathbb{C}^{\mathcal{D}}, j \in \mathbb{J}\,. \tag{6d}$$

This in turns motivates to restrict the attention to levels of robustness in the range $[0,\ \bar{\eta}]$.

In response to this observed demand deviation, the R-ETEM in Aliakbarisani et al. (2020) assumes that the planner is able to adjust his procurement decisions. The chronology of decision making is presented in Figure 2 and the general formulation of R-ETEM can be summarized as follows:

$$\min_{\boldsymbol{x},\{\boldsymbol{y}_i(\cdot),\boldsymbol{s}_i\}_{i=1}^{|\mathbb{I}|}} \quad \max_{\{\boldsymbol{\zeta}_i\in\mathcal{Z}_i(\Gamma_i)\}_{i=1}^{|\mathbb{I}|}} f^\top \boldsymbol{x} + \sum_{i\in\mathbb{I}} h_i^\top \boldsymbol{y}_i(\boldsymbol{\zeta}_i) \tag{7a}$$

$$\text{s.t.} \quad A_i\boldsymbol{x} + E_i\boldsymbol{s}_i + B_i\boldsymbol{y}_i(\boldsymbol{\zeta}_i) \leq b_i + C_i\boldsymbol{\zeta}_i \quad \forall \boldsymbol{\zeta}_i \in \mathcal{Z}_i(\Gamma_i),\ \forall i \in \mathbb{I} \tag{7b}$$

$$F_i\boldsymbol{s}_i \leq U_i,\ \boldsymbol{s}_i \geq 0 \quad \forall i \in \mathbb{I} \tag{7c}$$

$$D\boldsymbol{x} \leq e\,, \tag{7d}$$

where $\mathcal{Z}_i(\Gamma_i) := \{\boldsymbol{\zeta}_i \,|\, \|\boldsymbol{\zeta}_i\|_\infty \leq 1,\ \|\boldsymbol{\zeta}_i\|_1 \leq \Gamma_i\}$, $\Gamma_i = \sqrt{|\mathbb{S}^j| \times |\mathbb{C}^U| \times |\mathbb{L}|}$ with $i = (t,j)$, and where the seasonal procurement variable $\boldsymbol{y}_i(\cdot)$ is adjustable with respect to the realized uncertain parameter in the same time period and season $\boldsymbol{\zeta}_i$. Because such a multi-stage robust optimization problem is generally intractable (see Ben-Tal et al. 2004), Aliakbarisani et al. (2020) proposes a conservative approximation where the adjustable variable $\boldsymbol{y}_i(\boldsymbol{\zeta}_i)$ are affine functions of $\bar{\boldsymbol{\zeta}}_i$, i.e., $\boldsymbol{y}_i(\boldsymbol{\zeta}_i) = \boldsymbol{y}_i + \boldsymbol{Y}_i\bar{\boldsymbol{\zeta}}_i$, where $\boldsymbol{y}_i$ and $\boldsymbol{Y}_i$ become the decision variables, and $\bar{\boldsymbol{\zeta}}_i \in \bar{\mathcal{Z}}_i$ is a lifted representation of $\boldsymbol{\zeta}_i$ that distinguishes between positive and negative deviations and such that $\mathcal{Z}_i(\Gamma_i) = P_i\bar{\mathcal{Z}}_i$ for some projection matrix P_i. The final conservative approximation of the R-ETEM takes the form:

$$\min_{\boldsymbol{x},\{\boldsymbol{y}_i,\boldsymbol{Y}_i,\boldsymbol{s}_i\}_{i=1}^{|\mathbb{I}|}} \quad \max_{\{\bar{\boldsymbol{\zeta}}_i\in\bar{\mathcal{Z}}_i\}_{i=1}^{|\mathbb{I}|}} f^\top \boldsymbol{x} + \sum_{i\in\mathbb{I}} h_i^\top (\boldsymbol{y}_i + \boldsymbol{Y}\bar{\boldsymbol{\zeta}}_i) \tag{8a}$$

$$\text{s.t.} \quad A_i\boldsymbol{x} + E_i\boldsymbol{s}_i + B_i(\boldsymbol{y}_i + \boldsymbol{Y}\bar{\boldsymbol{\zeta}}_i) \leq b_i + C_iP_i\bar{\boldsymbol{\zeta}}_i \quad \forall \bar{\boldsymbol{\zeta}}_i \in \bar{\mathcal{Z}}_i,\ \forall i \in \mathbb{I} \tag{8b}$$

$$F_i\boldsymbol{s}_i \leq U_i,\ \boldsymbol{s}_i \geq 0 \quad \forall i \in \mathbb{I} \tag{8c}$$

$$D\boldsymbol{x} \leq e\,, \tag{8d}$$

After applying standard robust reformulation technique, problem (7) is conservatively approximated using a single finite-dimensional linear program that can be solved using either off-the-shelf solvers, or more efficiently using a Bender's decomposition scheme. We refer interested readers to Aliakbarisani et al. (2020) for more technical details and to Appendix B for a formal summary of the differences between R-ETEM and the robust model proposed in Babonneau and Haurie (2019).

4 A behavioral model for exchangeable EVs

Inspired by Tchuendom et al. (2019), we employ a LQG to model the charging/discharging behavior of a fleet of N exchangeable EVs. Each EV user is a price taker, but the aggregated charging profile affects the real time electricity price. EV users choose their charging profile rationally (i.e. they seek to minimize a given cost function). The cost function, beside the price of energy consumption, takes into account that i) EV users have a preferable state of the charge during the day, and any deviation from it is costly, and ii) EV users want to protect their batteries from the consequences of fast charging. Therefore the cost function is the summation of energy price, cost of deviation from the Desired Level of Charge (DLC) and cost of fast charging. In the limit as the fleet's size N goes to infinity, the LQG becomes a Mean Field Game (MFG) model. MFG theory is a well known technique to study the strategic behavior of large population of exchangeable interacting agents and can be used to approximate the solution of the LQG model when N is large.

4.1 Linear quadratic game formulation

Consider a N-player stochastic game of exchangeable EV users who want to charge their batteries in a finite horizon ($T > 0$) at minimum cost. We consider $T = 1$ represents one day, $\tau \in [0, T]$ is the continuous index for all time slots inside this day. It is assumed that the discharge profile i.e., $(\nu_\tau)_{\tau\in[0,T]}$, is estimated from the mobility data and exogenously given to the model, and it is common to all EV users. But, vehicle specific Brownian motions, i.e., $W^i := (W^i_\tau)_{\tau\in[0,T]}, i \in \{1, \ldots, N\}$, account for driver to driver independent idiosyncratic deviations from the common discharge profile.

Every EV user's control consists in the amount of charge applied at time τ denoted by $(u^i_\tau)_{\tau\in[0,T]}, i \in \{1, \ldots, N\}$. Also, the process $(X^i_\tau)_{\tau\in[0,T]}, i \in \{1, \ldots, N\}$ denotes fleet's states of charge which dynamics are captured by the following linear stochastic system of equations:

$$X^i_\tau = x_0 + \int_0^\tau (u^i_r - v_r)dr + \varepsilon W^i_\tau \quad \forall i \in \{1, \ldots, N\}, \tau \in [0, T],$$

where ε is a strictly positive constant and the initial state x_0 is a random parameter with a normal distribution $\mathcal{N}(a_0, s^2)$. We also denote by a_τ the preferrable/comfortable state of the charge profile common to all agents, which is exogenously defined.

Because the EV users are exchangeable, we can highlight a representative EV user, which we identify by $i \in \{1, .., N\}$. The study of the finite behavioral game model is formulated as a stochastic linear system with quadratic cost function, reveals that, any rationally chosen control by the representative EV user must be an affine function of its state of the charge process, which is modelled as a Gaussian process. Thus, thanks to the Gaussian nature of the state of charge, the control process u^i_τ, for any $i \in \{1, .., N\}$, and their sample mean process, will also be Gaussian.

Given the set of N players control processes, one can define the sample mean of the finite fleet of EVs, denoted $\Delta^N(U_\tau)$, where $U_\tau := \{u^i_\tau, i = 1, \dots, N\}$, as:

$$\Delta^N(U_\tau) := \frac{1}{N}\sum_{i=1}^{N} u^i_\tau, \quad \forall \tau \in [0, T].$$

The finite behavioral game model assumes that the charging/discharging marginal price is a function of the fleet's aggregate demand profile through its mean demand as below:

$$p_\tau := \lambda(\tau)\Delta^N(U_\tau),\ \forall \tau \in [0, T], \tag{9}$$

where $\lambda : [0,\ T] \to [0,\ \infty)$ is a function, smooth outside of a set of measure zero. (Note that, we consider functions that are smooth outside of a set of measure zero because we will solve the associated MFG model numerically).

Given the fixed marginal price function defined above, each player $i = 1, \dots, N$ minimizes the following cost function:

$$J^i(u^i, u^{-i}) = \mathbb{E}\Big[\frac{\overline{q}}{2}(X^i_T - a_T)^2 + \int_0^T \Big(\frac{\kappa}{2}(u^i_\tau)^2 + u^i_\tau p_\tau + \frac{q}{2}(X^i_\tau - a_\tau)^2\Big)d\tau\Big]. \tag{10}$$

Observe that the cost function of any player $i \in \{1, .., N\}$ depends on the controls of all other players, denoted $u^{-i} := (u^1, \dots, u^{i-1}, u^{i+1}, \dots, u^N)$, through the marginal price which is a function of the fleet's aggregate demand profile.

In the cost function, the constants $\overline{q} > 0$ and $q > 0$ model the cost associated to the deviation from the desired level of charge $(a_\tau)_{\tau\in[0,T]}$, and the term $\frac{\kappa}{2}(u^i_\tau)^2$ represents the cost of battery deterioration from fast charging/discharging. Even in this linear quadratic Gaussian setting, finding a Nash equilibrium to such a behavioral game model quickly becomes intractable as the number of players increases.

4.2 Mean field game formulation and solvability

To circumvent the problem that finding the Nash equilibrium in the formulated linear quadratic game becomes intractable when N becomes very large, we consider the MFG model as a method to find an approximate Nash equilibrium, for which the approximation error decreases as N goes to infinity. In a nutshell, the solution of a MFG model, referred to as a MFG equilibrium corresponds to the exact Nash equilibrium of the game with infinitely many players.

We define a Brownian motion $(W_\tau)_{\tau\in[0,T]}$ on a complete probability space denoted $(\Omega, \mathbb{F} = (\mathcal{F}_\tau)_{\tau\in[0,T]}, \mathbb{P})$ satisfying the usual conditions, where, $\mathcal{F}_\tau = \sigma\{x_0, W_s,\ 0 \le s \le \tau\}$, defines the filtration at time $\tau \in [0, T]$. Consider the set of admissible controls, denoted by $\mathcal{A}([0, T])$, below:

$$\mathcal{A}([0,T]) = \Big\{x : \Omega \times [0,T] \longrightarrow \mathbb{R} \quad | \quad \mathbb{E}\Big[\int_0^T |x_t|^2 dt\Big] < \infty\Big\}. \tag{11}$$

Below, we define the mean field game associated to the finite behavioral game model above, in three steps :

1. Fix a candidate average aggregate (mean) demand profile $\Delta := (\Delta_\tau)_{\tau\in[0,T]}$
2. Solve the control problem of finding $u^* \in \mathcal{A}([0, T])$ such that it is a minimizer of:

$$\min_{u\in\mathcal{A}([0,T])} \mathbb{E}\Big[\frac{\overline{q}}{2}(X_T - a_T)^2 + \int_0^T \Big(\frac{\kappa}{2}(u_\tau)^2 + u_\tau p_\tau(\Delta_\tau) + \frac{q}{2}(X_\tau - a_\tau)^2\Big)d\tau\Big], \tag{12}$$

where, $p_\tau(\Delta) := \lambda(\tau)\Delta_\tau$, and

$$X_\tau = x_0 + \int_0^\tau (u_s - v_s)ds + \varepsilon W_\tau, \quad x_0 = \mathcal{N}(a_0, s^2).$$

3. Show that, the MFG equilibrium is achieved. That is:

$$\Delta_\tau := \mathbb{E}[u_\tau^*], \ \forall \tau \in [0, T]. \tag{13}$$

Observe that the MFG model defined above consists of a control problem coupled with a fixed-point problem. The MFG equilibrium, denoted by $(u_\tau^*, \Delta_\tau)_{\tau\in[0,T]}$, is composed of the optimal demand profile of the representative player and the mean demand profile of the infinite population of players.

The following theorem, recalled from Tchuendom et al. (2019), characterizes the solution to the mean field game defined above.

Theorem 1. *There is a solution $(u_\tau^*, \Delta_\tau)_{\tau\in[0,T]}$ to the mean field game defined above if and only if there is a solution $(\eta_\tau, w_\tau, \Phi_\tau, \Delta_\tau)_{\tau\in[0,T]}$ for the following Forward-Backward Ordinary Differential Equations (FBODE):*

$$\frac{d\eta_\tau}{d\tau} = \frac{\eta_\tau^2}{\kappa} - q, \ \eta_T = \overline{q}, \tag{14}$$

$$\frac{dw_\tau}{d\tau} = \Big(\frac{\varepsilon^2\eta_\tau^2}{\kappa^2} - \frac{2q}{\eta_\tau}w_\tau\Big), \ w_0 = \frac{s^2\eta_0^2}{\kappa^2}, \tag{15}$$

$$\frac{d\Delta_\tau}{d\tau} = -F_1(\tau)\Phi_\tau - F_2(\tau)\Delta_\tau + F_3(\tau), \tag{16}$$

$$\frac{d\Phi_\tau}{d\tau} = B_1(\tau)\Phi_\tau + B_2(\tau)\Delta_\tau + B_3(\tau), \tag{17}$$

$$\Delta_0 = I_1(0)\Phi_0 + I_2(0), \ \Phi_T = -\overline{q}a_T. \tag{18}$$

The coefficients of the FBODEs are defined as:

$$I_1(\tau) = \frac{-1}{\kappa + \lambda(\tau)}, \qquad I_2(\tau) = -I_1(\tau)\Big(\eta_\tau(sF^{-1}[0.5; 0, 1] - a_0)\Big),$$

$$B_1(\tau) = \frac{\eta_\tau}{\kappa}, \quad B_2(\tau) = \frac{\eta_\tau\lambda(\tau)}{\kappa}, \quad B_3(\tau) = qa_\tau + \frac{\eta_\tau(\kappa v_\tau)}{\kappa},$$

$$F_1(\tau) = -\frac{q}{\eta_\tau}I_1(\tau), \quad F_2(\tau) = -I_1(\tau)\Big(\frac{d\lambda(\tau)}{d\tau} + \frac{q}{\eta_\tau}[\lambda(\tau) + \kappa]\Big),$$

$$F_3(\tau) = -\kappa I_1(\tau)\Big(\frac{\varepsilon^2\eta_\tau^2 F^{-1}[0.5; 0, 1]}{2\kappa^2\sqrt{w_\tau}} - \frac{q}{\kappa}[a_\tau + \frac{\lambda(\tau)}{\eta_\tau}]\Big).$$

where $F[r; 0, 1]$ denotes the Cumulative Distribution Function of a standard normal random variable with mean 0 and variance 1.

Theorem 1 states that solving the mean field game above is equivalent to solving the FBODEs (14-15-16-17). Existence and uniqueness of solutions to the FBODEs (14-15-16-17), is garanteed under contraction type conditions (see Tchuendom et al. (2019)).

We recall that in this setting, the process $(u_\tau^*)_{\tau\in[0,T]}$ denotes to the optimal demand of the representative EV user at equilibrium and $(\Delta_\tau)_{\tau\in[0,T]}$ denotes the average optimal demand of all EV users at equilibrium (i.e $\Delta_\tau = \mathbb{E}[u_\tau^*], \ \tau \in [0, T]$).

Thanks to the linear-quadratic nature of the control problem, the optimal state of the charge and demand of the representative EV user at equilibrium $(u^*_\tau)_{\tau\in[0,T]}$, is given by the feedback formula below:

$$X^*_\tau = x_0 - \int_0^\tau \frac{1}{\kappa}\big[\eta_r X^*_r + \Phi_r + \lambda(r)\Delta_r + \kappa v_r\big]dr + \varepsilon W_\tau, \quad \tau \in [0,T], \tag{19}$$

$$u^*_\tau = -\frac{1}{\kappa}\big[\eta_\tau X^*_\tau + \Phi_\tau + \lambda(\tau)\Delta_\tau\big], \quad \tau \in [0,T]. \tag{20}$$

We note that, solving the FBODEs (14-15-16-17) is not straightforward, even in our linear setting. The difficulty stems from the fact that the associated initial and terminal conditions. Observe that, the initial mean demand profile (Δ_0) depends on the initial value (Φ_0), which is not available at time $\tau = 0$. To circumvent this difficulty, the following proposition exploits the linear structure of the FBODEs (14-15-16-17), to obtain a representation of the deterministic profile $(\Phi_\tau)_{\tau\in[0,T]}$ as a linear function of the average optimal demand of EV users, $(\Delta_\tau)_{\tau\in[0,T]}$.

Proposition 2. *Assume that there is a unique solution, $(\eta_\tau, w_\tau, \Phi_\tau, \Delta_\tau)_{\tau\in[0,T]}$, to the the FBODEs (14-15-16-17) and a unique solution $(\Psi_\tau, \Pi_\tau)_{\tau\in[0,T]}$, to the backwards ordinary differential equations (BODEs) below: $\forall\tau[0,T]$*

$$\frac{d\Psi_\tau}{d\tau} = F_1(\tau)\Psi^2_\tau + F_2(\tau)\Psi_\tau + B_1(\tau)\Psi_\tau + B_2(\tau), \quad \Psi_T = 0, \tag{21}$$

$$\frac{d\Pi_\tau}{d\tau} = F_1(\tau)\Psi_\tau\Pi_\tau - F_3(\tau)\Psi_\tau + B_1(\tau)\Pi_\tau + B_3(\tau), \quad \Pi_\tau = -\bar{q}a_T, \tag{22}$$

then, the following representation formula holds:

$$\Phi_\tau = \Psi_\tau\Delta_\tau + \Pi_\tau, \quad \forall\tau \in [0,T]. \tag{23}$$

Proof. We prove the proposition by applying a chain differentiation rule to representation formula (23) and obtaining the ODE (17).

$$\begin{aligned}
\frac{d\Phi_\tau}{d\tau} &= \Delta_\tau\frac{d\Psi_\tau}{d\tau} + \Psi_\tau\frac{d\Delta_\tau}{d\tau} + \frac{d\Pi_\tau}{d\tau} \quad \forall\tau \in [0,T],\\
&= \Delta_\tau\Big[F_1(\tau)\Psi^2_\tau + F_2(\tau)\Psi_\tau + B_1(\tau)\Psi_\tau + B_2(\tau)\Big]\\
&\quad + \Psi_\tau\Big[-F_1(\tau)(\Psi_\tau\Delta_\tau + \Pi_\tau) - F_2(\tau)\Delta_\tau + F_3(\tau)\Big]\\
&\quad + \Big[F_1(\tau)\Psi_\tau\Pi_\tau - F_3(\tau)\Psi_\tau + B_1(\tau)\Pi_\tau + B_3(\tau)\Big], \quad \forall\tau \in [0,T],\\
&= B_1(\tau)\Phi_\tau + B_2(\tau)\Delta_\tau + B_3(\tau), \quad \forall\tau \in [0,T],
\end{aligned}$$

and at terminal condition, $\tau = T$, we have:

$$\Phi_T = \Psi_T\Delta_T + \Pi_T = 0 \times \Delta_T + (-\bar{q}a_T) = -\bar{q}a_T. \qquad \square \tag{24}$$

$\square$

As a direct consequence of the proposition 2, and equation (20), the representative EV user's optimal demand at equilibrium can be rewritten as follows:

$$u^*_\tau = -\frac{1}{\kappa}\big[\eta_\tau X^*_\tau + \Phi_\tau + \lambda(\tau)\Delta_\tau\big], \quad \forall\tau \in [0,T], \tag{25}$$

$$= -\frac{1}{\kappa}\big[\eta_\tau X^*_\tau + (\Psi_\tau \Delta_\tau + \Pi_\tau) + \lambda(\tau)\Delta_\tau\big], \quad \forall \tau \in [0,T]. \tag{26}$$

From this updated formula for the representative EV user's optimal demand, we can derive another formula for the representative EV user's mean optimal demand.

Indeed, since at MFG equilibrium it holds that $\mathbb{E}[u^*_\tau] = \Delta_\tau,\ \forall \tau \in [0,T]$, it follows that:

$$\begin{aligned}
&\Delta_\tau = \mathbb{E}[u^*_\tau],\ \forall \tau \in [0,T], \\
&\qquad \iff \Delta_\tau = -\frac{1}{\kappa}\bigg[\eta_\tau \mathbb{E}[X^*_\tau] + (\Psi_\tau + \lambda(\tau))\Delta_\tau + \Pi_\tau\bigg],\ \forall \tau \in [0,T], \\
&\qquad \iff \Delta_\tau\big(-\kappa - \Psi_\tau - \lambda(\tau)\big) = \eta_\tau \mathbb{E}[X^*_\tau] + \Pi_\tau,\ \forall \tau \in [0,T], \\
&\qquad \iff \Delta_\tau = -\frac{\eta_\tau \mathbb{E}[X^*_\tau] + \Pi_\tau}{\kappa + \Psi_\tau + \lambda(\tau)},\ \forall \tau \in [0,T],
\end{aligned} \tag{27}$$

where the process $\big(\mathbb{E}[X^*_\tau]\big)_{\tau\in[0,T]}$ denotes the EV users' average optimal state of charge :

$$\begin{aligned}
\mathbb{E}[X^*_\tau] &= \mathbb{E}[x_0] - \int_0^\tau \frac{1}{\kappa}\bigg[\eta_r \mathbb{E}[X^*_r] - \big(\Psi_r + \lambda(r)\big)\frac{\eta_r \mathbb{E}[X^*_r] + \Pi_r}{\kappa + \Psi_r + \lambda(r)} + \Pi_r + \kappa v_r\bigg] dr \\
&= \mathbb{E}[x_0] - \int_0^\tau \bigg[\frac{\eta_r \mathbb{E}[X^*_r] + \Pi_r}{\kappa + \Psi_r + \lambda(r)} + v_r\bigg] dr, \quad ,
\end{aligned} \tag{28}$$

for all $\tau \in [0,\ T]$.

Finally, to compute the EV users' average optimal state of charge and average demand, it is enough to compute the solution, (η_τ, w_τ) to FBODEs $(14-15)$, and the solution, $(\Psi_\tau, \Pi_\tau)_{\tau\in[0,T]}$, to the FBODEs $(21-22)$. Then evaluate the feedback formulas (28) and (27). A detailed implementation algorithm is presented in Appendix C.

5 Coupling R-ETEM and LQGs

Up to this point, we have proposed a R-ETEM model that immunizes the expansion plan against possible behavioral deviations from the planned response over a 40+ years horizon. We also presented a linear quadratic game that can be used to simulate the continuous time charging behavior of EV users on a typical day. Focusing on the case where EV charging is the only useful demand with behavioral uncertainty (i.e. $\mathbb{C}^U := \{\bar{c}\}$ with $\bar{c}$ as electricity used to charge EVs, we are left with the task of describing the interactions between the two types of models. Specifically, for each time-season $i \in \mathbb{I}$ and region $l \in \mathbb{L}$, one can envision having recourse to the linear quadratic game formulation to simulate the behaviour of EV users on a typical day of this period based on available information regarding N, a, q, and κ. In doing so, we first will ensure that the price function used in the LQG is consistent with the market clearing price (i.e. marginal cost) implied by the solution of R-ETEM. We will also propose a bisection algorithm that calibrates the level of uncertainty in R-ETEM in a way that ensures R-ETEM produces a robust expansion plan that is behaviorally-consistent with the LQG models. In simple terms, the final robust plan should be immunized against the demand response deviations observed in the ensemble of behavioral model when it is implemented.

5.1 Extracting the marginal cost in R-ETEM

In this subsection, we indicate how to extract marginal costs for the procurement of useful energy $c \in \mathbb{C}^{\mathcal{D}}$. In particular, in the deterministic model (1), this can be done by looking at the dual variable

associated to the demand satisfaction constraint (2). In the conservative approximation of R-ETEM, this is not as straightforward. This section proposes a general procedure for doing so.

Specifically, we start by observing that (8) can be equivalently formulated as:

$$\min_{\boldsymbol{x},\{\boldsymbol{y}_i,\boldsymbol{Y}_i,\boldsymbol{s}_i,\bar{\boldsymbol{s}}_i\}_{i=1}^{|\mathbb{I}|}} \max_{\{\bar{\boldsymbol{\zeta}}_i\in\bar{\mathcal{Z}}\}_{i=1}^{|\mathbb{I}|}} f^\top \boldsymbol{x} + \sum_{i\in\mathbb{I}} h_i^\top(\boldsymbol{y}_i + \boldsymbol{Y}\bar{\boldsymbol{\zeta}}_i) \tag{29a}$$

$$\text{s.t.} \quad A_i\boldsymbol{x} + E_i\boldsymbol{s}_i + B_i(\boldsymbol{y}_i + \boldsymbol{Y}\bar{\boldsymbol{\zeta}}_i) \le b_i + C_iP_i\bar{\boldsymbol{\zeta}}_i \quad \forall\bar{\boldsymbol{\zeta}}_i\in\bar{\mathcal{Z}}_i,\ \forall i\in\mathbb{I} \tag{29b}$$

$$F_i\bar{\boldsymbol{s}}_i \le U_i,\ \bar{\boldsymbol{s}}_i \ge 0 \quad \forall i\in\mathbb{I} \tag{29c}$$

$$D\boldsymbol{x} \le e\,, \tag{29d}$$

$$\boldsymbol{s}_i = \bar{\boldsymbol{s}}_i \quad \forall i\in\mathbb{I} \tag{29e}$$

Recall that $\boldsymbol{s}_i$ was capturing all the relative demand responses $\boldsymbol{V}_{t,s,l,c}$ with $i=(t,j)$, $s\in\mathbb{S}_j$, and $c\in\mathbb{C}^{\mathcal{D}}$. Hence, when the minimum of problem (29) is finite, the optimal assignment $\{\boldsymbol{\gamma}_i^*\}_{i\in\mathbb{I}}$ of dual variables associated to (29e) captures the marginal effect of increasing the relative demand responses on the optimal cost. We are left with converting marginal cost of relative demand response in units of marginal cost of absolute demand response. In particular, the marginal energy cost for final demand c, in region l, in time period t and time-slice s according to the conservative R-ETEM model (8) is $\bar{\gamma}^*_{t,s,l,c} := [\boldsymbol{\gamma}_i^*]_{t,s,l,c}/\Theta_{t,l,c}$ with $i=(t,j) : s\in\mathbb{S}^j$, and where $[\boldsymbol{\gamma}_i^*]_{t,s,l,c}$ takes the element of the dual vector associated to constraint $\boldsymbol{V}_{t,s,l,c} = \bar{\boldsymbol{V}}_{t,s,l,c}$.

5.2 Calibrating the marginal price function in MFG

In order to calibrate the price function in the MFG behavioral model, we employ a similar approach as in Babonneau et al. (2020). Namely, the marginal price p_τ should reflect the marginal cost of production when the average charging amount is equal to the planned response. In time-season period $i=(t,j)$, and for region l, this is done using:

$$\lambda^{i,l}(\tau) := \sum_{s\in\mathbb{S}^j} \mathbf{1}\{\tau\in\mathcal{T}_s\}\frac{\bar{\gamma}^*_{t,s,l,\bar{c}}}{\Theta_{t,l,\bar{c}}\boldsymbol{V}_{t,s,l,\bar{c}}/(N^l D_i)} \tag{30}$$

where $\mathbf{1}\{\cdot\}$ is the indicator function, N^l is the number of vehicles in region l, $\bar{c}$ is the index of the final demand of electricity for charging EVs, $\mathcal{T}_s$ indicates the period of the day associated to time slice s, and where D_i is the total number of days in time-season period $i=(t,j)$, Indeed, one can check that with this definition if for any $\tau\in\mathcal{T}_s$ we have that the average charging amount and the planned response are the same, i.e. $\Delta^N(U_\tau) = \Theta_{t,l,\bar{c}}\boldsymbol{V}_{t,s,l,\bar{c}}/(ND_i)$, then it follows that the marginal price reduces to:

$$\begin{aligned} p_\tau &= \lambda^{i,l}(\tau)\Delta^N(U_\tau) = \lambda^{i,l}(\tau)\,\Theta_{t,l,\bar{c}}\boldsymbol{V}_{t,s,l,\bar{c}}/(ND_i) \\ &= \sum_{s'\in\mathbb{S}^j} \mathbf{1}\{\tau\in\mathcal{T}_{s'}\}\bar{\gamma}^*_{t,s',l,\bar{c}} = \bar{\gamma}^*_{t,s,l,\bar{c}}\,. \end{aligned}$$

5.3 Optimizing behaviorally-consistent robust expansion plans

Once the marginal price functions used in each LQG are well calibrated, the question remains of whether the behavioral uncertainty that is modeled in R-ETEM is consistent with the simulations produced by the behavioral LQG models. A very natural condition to impose on R-ETEM is that it should produce a plan, which once implemented leads to consumers behaviors that fall within the range for which the plan is immunized against.

Definition 1. *The optimal robust expansion strategy $\boldsymbol{x}^*$ and planned demand response $\boldsymbol{s}^*$ are "behaviorally-consistent" if when the operator charges consumers according to the price function* (9)*, the actual relative demand response deviation measured by the behavioral model of Section 4 falls within the uncertainty set $\Xi(\eta)$ defined in* (5)*.*

Practically speaking, given any fixed uncertainty set $\Xi(\eta)$, verifying whether $\boldsymbol{x}^*(\eta)$ and $\boldsymbol{s}^*(\eta)$, i.e. the optimal solutions of problem (8) under $\Xi(\eta)$, are behaviorally-consistent involves solving the MFGs for each $i \in \mathbb{I}$ and $l \in \mathbb{L}$ with the price function (9), obtaining $\Delta^{i,l}$ based on equation (27) and verifying whether the realized relative demand vector $\hat{\boldsymbol{s}}$ defined as:

$$[\hat{\boldsymbol{s}}_i]_{t,s,l,\bar{c}} := \frac{\int_{\tau \in \mathcal{T}_s} \Delta_\tau^{i,l} d\tau}{\sum_{s \in \mathcal{S}^j} \int_{\tau \in \mathcal{T}_s} \Delta_\tau^{i,l} d\tau}, \ \forall s \in \mathcal{S}^j, \ \forall l \in \mathbb{L}, \forall (t,j) = i, \ \forall i \in \mathbb{I}, \tag{31}$$

is such that $\boldsymbol{\delta} = \hat{\boldsymbol{s}} - \boldsymbol{s} \in \Xi(\eta)$.

Conceptually, our calibration procedure for η aims at finding the minimal worst-case cost expansion plan that is behaviorally-consistent with the LQG models. As such, given that the optimal value of problem (8) is non-decreasing in η, Algorithm 1 will equivalently aim at identifying the smallest level of robustness η that leads to a robust solution that is behaviorally consistent.

Lemma 3. *Algorithm 1 is guaranteed to terminate in $\log_2(\bar{\eta}/\varepsilon)$ iterations, where ε as the required level of precision and $\bar{\eta}$ the largest level of robustness considered (see equation* (6)*).*

Proof. This follows straightforwardly from the fact that Algorithm 1 is a bisection algorithm on interval $[0, \ \bar{\zeta}]$ that terminates when the interval has a length smaller than ε. □

Algorithm 1: A bisection algorithm to find a minimal worst-case optimal behaviorally-consistent expansion plan

Set a desired level of tolerance ε;
Set $\eta_{\text{LB}} = 0$, $\eta_{\text{UB}} = \bar{\eta}$;
while $\eta_{UB} - \eta_{LB} > \varepsilon$ **do**
    Set $\eta = (\eta_{\text{LB}} + \eta_{UB})/2$;
    Solve problem (29) with $\Xi(\eta)$ to obtain $\boldsymbol{s}^*$ and $\bar{\gamma}^*$;
    for $(i,l) \in \mathbb{I} \times \mathbb{L}$ **do**
        Set $\lambda^{i,l}(\tau)$ according to equation (30);
        Solve the MFG in Section 4 for region l and time-season period i using $\lambda^{i,l}(\tau)$ to obtain $\Delta^{i,l}$;
    end
    Set $\hat{\boldsymbol{s}}$ as defined in (31);
    if $\hat{\boldsymbol{s}} - \boldsymbol{s} \in \Xi(\eta)$ **then**
        $\eta_{\text{UB}} \leftarrow \eta$;
    else
        $\eta_{\text{LB}} \leftarrow \eta$;
    end
    Solve problem (29) with $\Xi(\eta_{\text{UB}})$ and return $\boldsymbol{x}^*$;
end

6 Case study and numerical results

The proposed approach to obtain robust behaviorally consistent expansion strategy is implemented on a realistic case study based on the energy system of the Arc Lémanique region (Cantons of Geneva and Vaud, in Switzerland). Studies show that by 2050 up to 70% of the total transportation demand in the region can potentially be satisfied by electric vehicles (Babonneau et al. 2017). ETEM covers three regional buses and 142 different technologies including central electricity and heat production and distributed energy resources. We model 21 types of final demands which are categorized into industrial, residential and transportation. Based on the optimum annual share of EVs in satisfying useful transportation demand reported in Babonneau et al. (2017), we have calculated the annual final demand for electricity to charge EVs. Figure 3 shows the reference energy system (RES) modeled by ETEM. All data regarding ETEM model is from Babonneau and Haurie (2019) and for a more detailed description of the energy system in the Arc Lémanique region, we refer interested readers to this paper.

The purpose of this numerical study is i) to estimate the level of contribution of EV users in demand response programs by a LQG models, and ii) to obtain the robust capacity expansion policies that are behaviorally consistent. To do so, first we calibrate the LQG model with our available data. Then using Algorithm 1 we calibrate $\Xi(\eta)$ in order to estimate the required level of uncertainty in the R-ETEM to have behaviorally consistent expansion policies. In addition, we perform a sensitivity analysis on the cost parameter q in the LQG model. Finally, we analyze the influence of demand response and demand response uncertainty on expansion strategies and asses the price of robustness.

6.1 Calibrating the LQG models

In order to calibrate the LQG models, we use the useful demand of transportation which is satisfied by EVs, optimally calculated in Babonneau and Haurie (2019), as the aggregated discharge. In other words, we fix the demand to the actual demand in the deterministic ETEM model. Then ETEM calculates the marginal cost of electricity production given the already available mix of technologies in the energy system. The marginal cost is passed to LQG model and we calibrate the range of LQG parameters, i.e., q, $\overline{q}$ and κ so that it replicates actual demand responses close to the aggregated discharge. Figure 4a represents the average charging and discharging of a EV users in the fleet in a specific season and region $(i, l) = (1, 1)$. The average state of charge (SOC) for this control is also presented in Figure 4b. After aggregating the results of the LQG models, Figure 5 compares the nominal versus actual (i.e. simulated using LQG models) DR for the base period in the model.

6.2 Algorithm convergence and q-sensitivity on a 15-years horizon

In this section, we illustrate the convergence of Algorithm 1 when R-ETEM considers a 15-years horizon from 2015 to 2030.

6.2.1 Algorithm convergence

Figure 6 displays the convergence of Algorithm 1 in terms of upper and lower bounds for the optimal level of uncertainty η^*. We observe that the algorithm converges after 6 iterations to within a tolerance of $\varepsilon = 0.01$ and that the optimal level of uncertainty is $\eta^* \approx 0.26$. It means that at optimum, the R-ETEM model needs to be immunized against a 26% deviation of the actual demand response from the planned demand response. We note that when $\eta < \eta^*$ the obtained policies are not behaviorally consistent, while for $\eta > \eta^*$ the model is too conservative thus leading to larger worst-case total cost

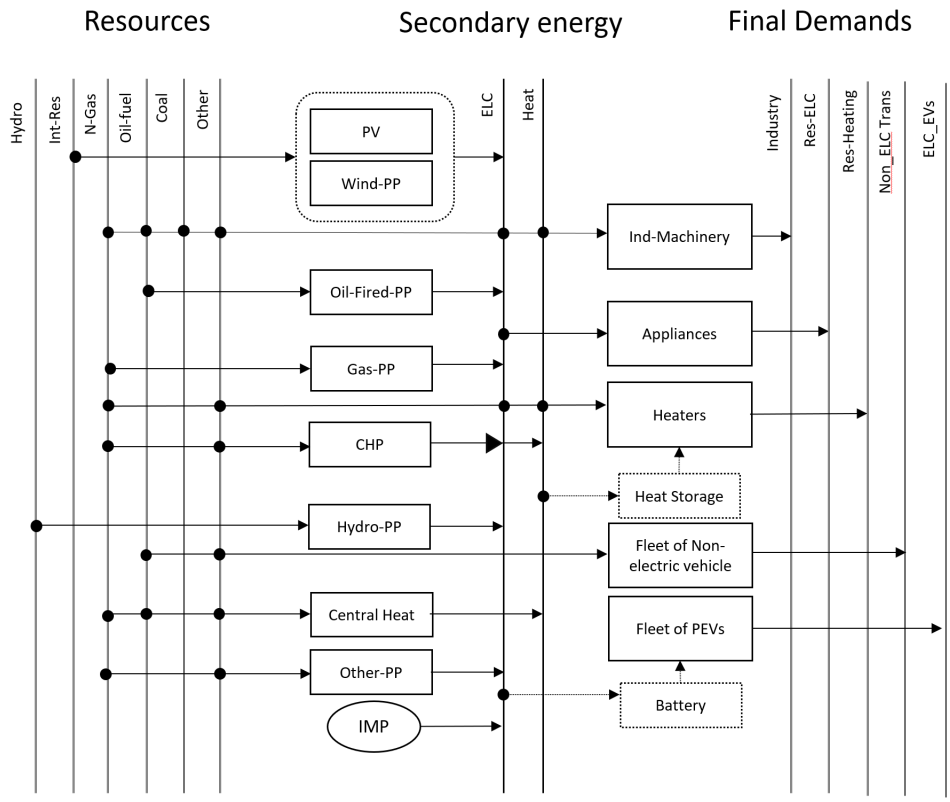

Figure 3: Arc Lémanique reference energy system, where Int-Res stands for intermittent resources (solar and wind), N-Gas for natural gas, Oil-fuel for processed oil products, Other for hydrogen and additional sources of energy (such as solid waste and wood and geothermal), ELC for electricity, RES for residential, PP for power plant, CHP for combined heat and power plant, IMP for electricity import, Ind-Machinery for industrial machinery. Other-PP includes geothermal, fuel-cell and municipal waste power plants. ELC_EVs is the perturbed useful demand (i.e. $\bar{c}$) for electricity to charge the battery of EVs.

than necessary. Therefore, when $\eta > \eta^*$, one can consider the optimal value of R-ETEM as an upper bound on the the minimal behaviorally consistent worst-case cost of the system, and similarly as a lower bound when $\eta < \eta^*$. These two bounds are presented in Figure 6.

6.2.2 Preliminary analysis of sensitivity to cost of deviation from DLC

In this section, we tested the sensitivity of the minimal behaviorally-consistent level of uncertainty η^*, and its associated worst case total cost of the system, with respect to the cost of deviation from the fleet desired level of charge (DLC) and present the results in Figure 7. When the cost of deviation from the DLC is higher, the minimal level of uncertainty is reduced. Indeed, when this cost is high, EV users are less responsive to the electricity price. In other words, they are willing to charge their battery at any price in order to reach their desired level of charge. In this situation, the charging behaviour becomes easier to predict based on mobility data. This in turns allows the model to employ a lower level of uncertainty in the planning phase.

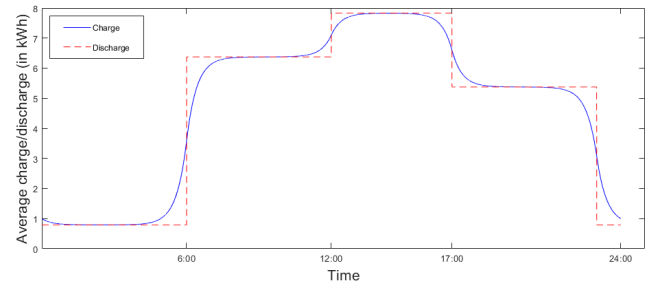

(a)

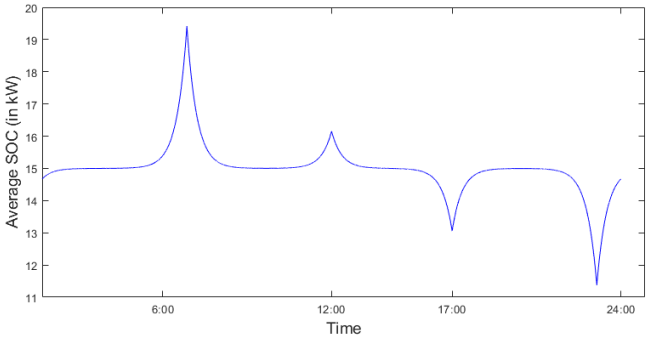

(b)

Figure 4: (a) Average charge and discharge and (b) average state of the charge (SOC) of batteries in the whole fleet for one day in a representative region and time period after LQG calibration.

6.3 Robustness of optimal capacity expansion plans for a 40-years horizon

In this section, we numerically show how robust behaviorally-consistent solutions affect the electricity generation capacities in the long-term R-ETEM covering 40 years from 2015 to 2055. Moreover, we compare the actual, planned and nominal DRs. Finally, we discuss the performance of robust behaviorally-consistent solutions.

6.3.1 Electricity generation capacity and planned DR

We now turn to studying the effect of accounting for demand response robustness on the capacity expansion strategy. Specifically, we will compare the strategies obtained for three different models: i) a model (referred to as No-DR) that assumes EV users do not participate in DR programs; (ii) a model (BI-DR) that assumes that EV users participate in DR programs and their contribution is fully predictable, hence is behaviorally inconsistent; and (iii) a model (RBC-DR) that assumes that EV users participate in DR programs and accounts for behavioral DR divergences. Numerically, the No-DR plan is obtained from solving (1) with $\nu_{t,s,l,c} = 0$ in constraint (3), the BI-DR plan is obtained from solving (1), and finally, the RBC-DR plan is obtained from solving (8) with η^* calibrated using Algorithm 1. Figure 8 shows the total installed capacity proposed by these three models. We observe that BI-DR installs the least amount of capacity compared to the other two models. This is because this model expects that peak loads will be significantly reduced using DR programs. By contrast, the No-DR is installing more gas power plant (around 39% more than BI-DR) to meet the peak load. Finally, RBC-DR builds extra capacity compared to BI-DR to immunize against deviations from planned EV user behaviors. The extra capacity is mostly provided by CHP technologies.

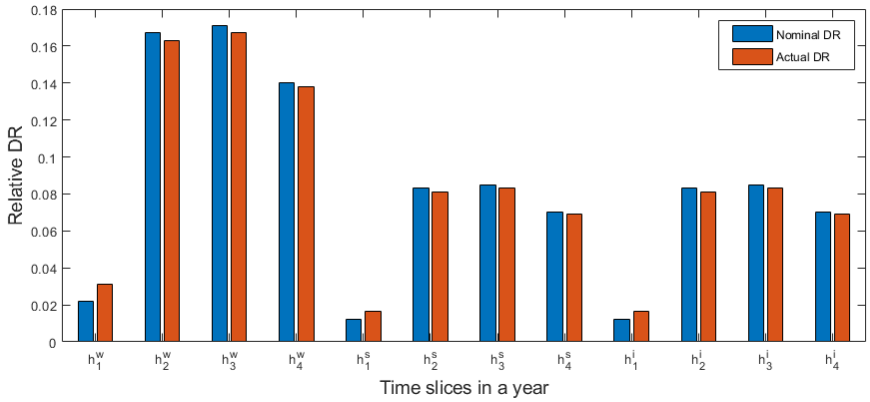

Figure 5: Actual versus nominal relative demand responses for all time slices in a year. h_1^w - h_4^w refer to four time slices in a winter day, h_1^s - h_4^s refer to four time slices in a summer day, and h_1^i - h_4^i refer to four time slices in a intermediate day (see table 1 for a definition of each time slice).

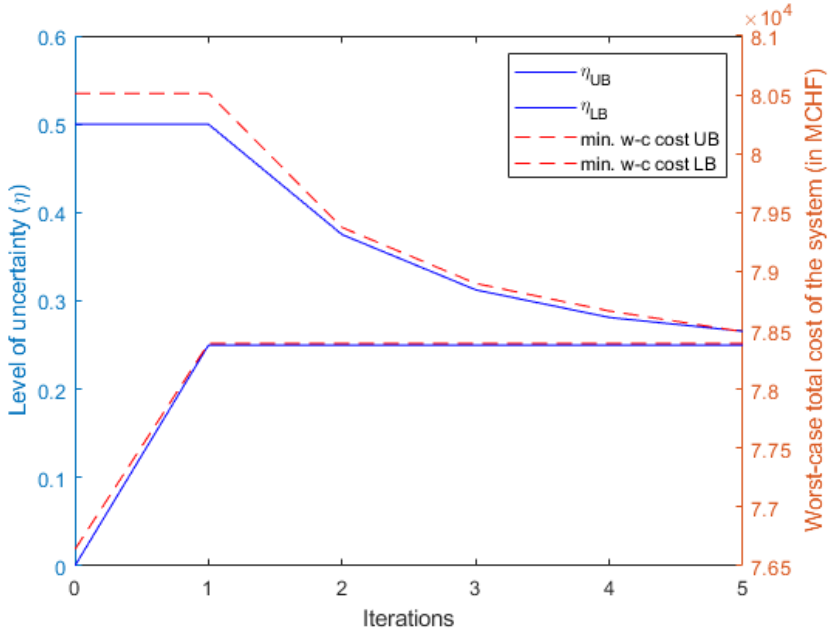

Figure 6: Convergence of the bisection algorithm (with $\varepsilon = 0.01$) in terms of the upper and lower bounds for the behaviorally-consistent level of uncertainty η (left axis) and the minimal worst-case total cost of the system (right axis).

Figure 9 compares the actual, planned and nominal DRs. The LQG model suggests, for all seasons, to charge more during time-slice h_1 (between 11:00 p.m. and 6:00 a.m.) as the marginal price of electricity is cheaper during these hours following lower network loads. Note that as the differences between the actual DR and the planned DR in all time-slices are always less that $\eta* \approx 0.26$, the expansion planning of the R-ETEM is indeed remains behaviorally consistent.

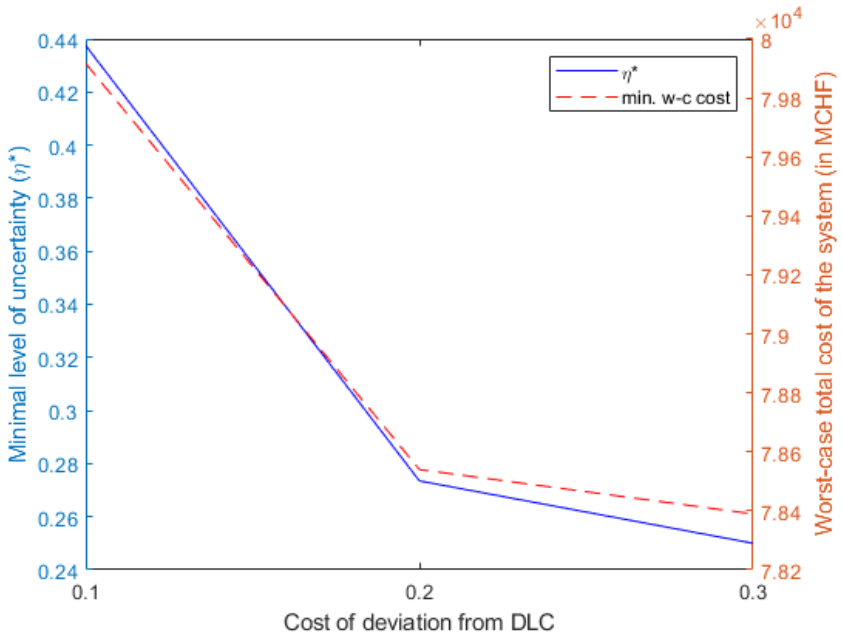

Figure 7: Sensitivity analysis of the minimal behaviorally-consistent level of uncertainty $\eta*$ (left axis) and and worst-case total cost of the system on the cost of deviation from the desired level of the charge (DLC).

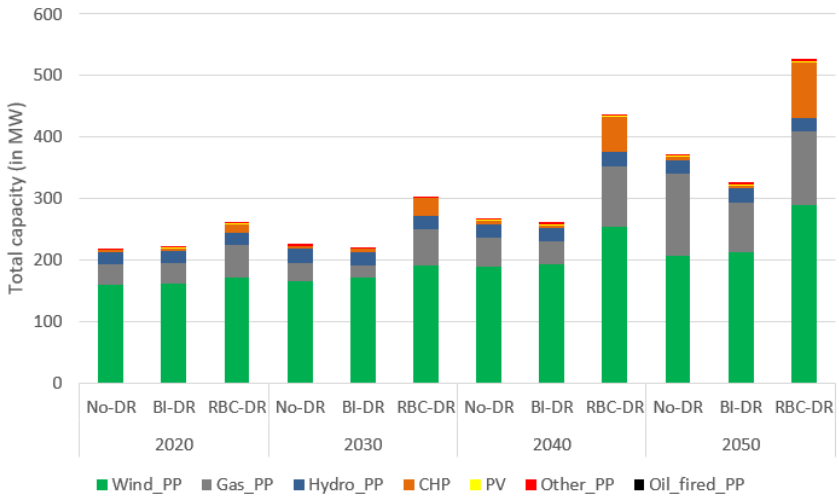

Figure 8: Evolution of the electricity generation capacity plan for 3 types of models: an optimal plan with no demand response (No-DR), an optimal plan with DR but behaviorally-inconsistent (BI-DR), and a robustly optimal behaviorally-consistent plan with DR (RBC-DR).

6.3.2 Robust performance

In this section, we evaluate the performance of the solutions of the three models introduced in Section 6.3.1, i.e., No-DR, BI-DR and RBC-DR. In doing so, we define two measures: i) the total cost of the system if we assume the scenario proposed by LQG happens (referred to as "actual cost"), and ii) the total cost of the system if we assume the planned DR happens with zero deviation (referred to as "nominal cost"). In order to obtain the actual and nominal costs, first we solve the

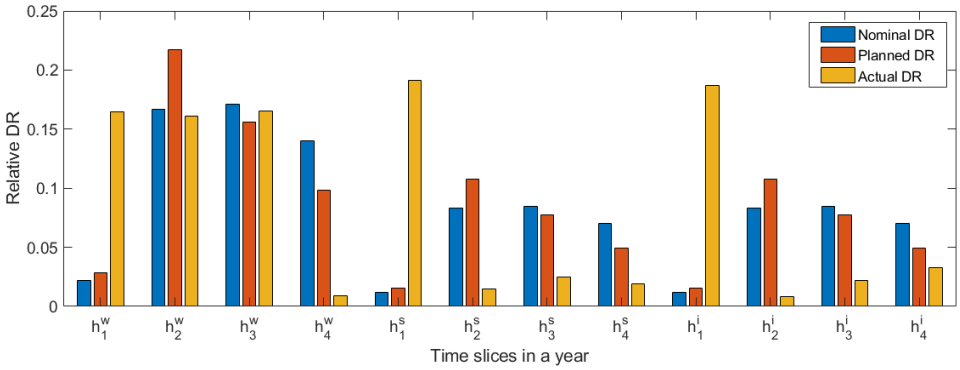

Figure 9: Nominal, actual and planned demand responses over all time-slices in a period. h_1^w to h_4^w refer to four time slices in a winter day, h_1^s to h_4^s refer to four time slices in a summer day, and h_1^i to h_4^i refer to four time slices in an intermediate day (see Table 1 for a definition of each time slice).

Table 2: Comparison of actual and nominal costs of No-DR, BI-DR and RBC-DR solutions.

	Actual cost MCHF	Rel diff[1] %	Nominal cost MCHF	Rel diff[1] %
RBC-DR	177,182.5	-	174,245.5	-
BI-DR	188,238.6	6.2%	170,328.3	-2.2%
No-DR	184,059.7	3.9%	170,931.5	-1.9%

[1] Relative difference with RBC-DR

three models and store the value of variable $\boldsymbol{x}$ and $\boldsymbol{s}_i$ in $(\boldsymbol{x}^{No-DR}, \boldsymbol{s}_i^{No-DR})$,$(\boldsymbol{x}^{BI-DR}, \boldsymbol{s}_i^{BI-DR})$, and $(\boldsymbol{x}^{RBC-DR}, \boldsymbol{s}_i^{RBC-DR})$. Then, we plug these values in problem (7) and re-optimize it fixing the value of $\boldsymbol{\zeta}_i$ to $\boldsymbol{s}_i - \hat{\boldsymbol{s}}_i$ and 0 for actual and nominal costs respectively. $\hat{\boldsymbol{s}}_i$ is the solution of LQG as is calculated in (31). Table 2 shows that RBC-DR reduces the actual cost of the system by 3.9% compared to No-DR model, and 6.2% compared to BI-DR model. Indeed, by installing more generation capacities (see again Figure 8), RBC-DR solutions are better protected against the realization of the actual DR calculated using the LQG models. But, in a case that there would be zero deviation between the actual DR and the planned DR, the cost of RBC-DR is 1.9% and 2.2% more than No-DR and BI-DR costs, respectively. This loss in performance under the nominal model can be interpreted as the price of robustness.

7 Conclusion

In this paper, we develop a robust approach to evaluate the interaction between electric vehicle (EV) users and utilities on a long-term generation expansion planning (GEP) problem for a smart grid. Namely, we employ a specific robust multi-period adjustable GEP problem, called R-ETEM, where the EV user demand responses are uncertain. In R-ETEM, one decides first on the optimal capacity expansion of the network and the planned demand responses. Then, on a seasonal basis, after observing the actual demand responses, the procurement decisions are taken. In our case study, we choose to immunize R-ETEM against perturbations of the demand response of a large fleet of EVs. To do so, we employ a linear quadratic game (LQG) to simulate the average charging behavior of the fleet. The utility broadcasts a real-time price which depends on the marginal cost of electricity

production (calculated by solving R-ETEM) and the aggregated charging demand of the fleet. In response, EV users minimize a cost function consisting of the price paid for electricity and the cost of deviation from a comfort zone. We propose a novel coupling algorithm between R-ETEM and the LQG with the purpose of adjusting the level of uncertainty in R-ETEM and obtaining behaviorally-consistent expansion plans. The coupling algorithm necessarily converges in finite iterations. We test our algorithm on a real-world case study based on the energy system of the "Arc Lémanique" region (Cantons of Geneva and Vaud, in Switzerland). The results reinforce that a behaviorally-consistent expansion plan can significantly reduce the total actual cost of the system (e.g., by 6.2% in our case study).

Acknowledgments. This research is supported by the Canadian IVADO program (VORTEX Project). Olivier Bahn and Erick Delage also both acknowledge the financial support from the Natural Sciences and Engineering Research Council of Canada (respectively RGPIN-2016-04214 and RGPIN-2016-05208). Rinel Foguen Tchuendom is supported by AFOSR grant FA 9550-19-1-0138. Finally, the authors are thankful to Frédéric Babonneau and Alain Haurie for providing the ETEM model used in Babonneau and Haurie (2019) and for their valuable discussions regarding the development of schemes that can couple the ETEM model with MFG approaches.

References

Aliakbarisani S, Bahn O, Delage E (2020) Affine decision rule approximation to immunize against demand response uncertainty in smart grids capacity planning. *Les Cahiers du GERAD* G–2020–62.

Babonneau F, Caramanis M, Haurie A (2016) A linear programming model for power distribution with demand response and variable renewable energy. *Applied Energy* 181:83 – 95.

Babonneau F, Caramanis M, Haurie A (2017) ETEM-SG: Optimizing regional smart energy system with power distribution constraints and options. *Environmental Modeling & Assessment* 22(5):411–430.

Babonneau F, Foguen R, Haurie A, Malhame R (2020) Coupling a power dispatch model with a wardrop or mean-field-game equilibrium model. *Dyn Games Appl* .

Babonneau F, Haurie A (2019) Energy technology environment model with smart grid and robust nodal electricity prices. *Annals of Operations Research* 274.

Ben-Tal A, Goryashko A, Guslitzer E, Nemirovski A (2004) Adjustable robust solutions of uncertain linear programs. *Mathematical Programming* 99(2):351–376.

Bloom JA (1983) Solving an electricity generating capacity expansion planning problem by generalized benders' decomposition. *Operations Research* 31(1):84–100.

Bloom JA, Caramanis M, Charny L (1984) Long-range generation planning using generalized benders' decomposition: Implementation and experience. *Operations Research* 32(2):290–313.

Chen Y, Bušić A, Meyn S (2014) Individual risk in mean field control with application to automated demand response. *53rd IEEE Conference on Decision and Control*, 6425–6432, ISSN 0191-2216, URL `http://dx.doi.org/10.1109/CDC.2014.7040397`.

Couillet R, Perlaza SM, Tembine H, Debbah M (2012) A mean field game analysis of electric vehicles in the smart grid. *2012 Proceedings IEEE INFOCOM Workshops*, 79–84, URL `http://dx.doi.org/10.1109/INFCOMW.2012.6193523`.

Dehghan S, Amjady N, Kazemi A (2014) Two-stage robust generation expansion planning: A mixed integer linear programming model. *IEEE Transactions on Power Systems* 29(2):584–597.

Gomes D, Saude J (2018) A mean-field game approach to price formation in electricity markets. *arXiv:1807.07088v1* .

Han D, Wu W, Sun W, Yan Z (2018) A two-stage robust stochastic programming approach for generation expansion planning of smart grids under uncertainties. *2018 IEEE Power Energy Society General Meeting (PESGM)*, 1–5.

Huang M, Malhamé RP, Caines PE (2006) Large population stochastic dynamic games: closed-loop McKean-Vlasov systems and the Nash certainty equivalence principle. *Commun. Inf. Syst.* 6(3):221–251, ISSN 1526-7555, URL `http://projecteuclid.org/euclid.cis/1183728987`.

Koltsaklis NE, Dagoumas AS (2018) State-of-the-art generation expansion planning: A review. *Applied Energy* 230:563 – 589.

Lasry JM, Lions PL (2006) Jeux à champ moyen. I. Le cas stationnaire. *C. R. Math. Acad. Sci. Paris* 343(9):619–625, ISSN 1631-073X, URL `http://dx.doi.org/10.1016/j.crma.2006.09.019`.

Lindholm L, Sandberg M, Szepessy A (2017) A mean field game model of an electricity market with consumers minimizing energy cost through dynamic battery usage URL `urn:nbn:se:kth:diva-214024`.

Lohmann T, Rebennack S (2017) Tailored benders decomposition for a long-term power expansion model with short-term demand response. *Management Science* 63(6):2027–2048.

Ma Z, Callaway DS, Hiskens IA (2013) Decentralized charging control of large populations of plug-in electric vehicles. *IEEE Transactions on Control Systems Technology* 21(1):67–78, ISSN 1063-6536, URL `http://dx.doi.org/10.1109/TCST.2011.2174059`.

Mejía-Giraldo D, McCalley J (2014) Adjustable decisions for reducing the price of robustness of capacity expansion planning. *IEEE Transactions on Power Systems* 29(4):1573–1582.

Mohsenian-Rad AH, Wong VWS, Jatskevich J, Schober R, Leon-Garcia A (2010) Autonomous demand-side management based on game-theoretic energy consumption scheduling for the future smart grid. *IEEE Transactions on Smart Grid* 1(3):320–331, URL `http://dx.doi.org/10.1109/TSG.2010.2089069`.

Tchuendom R, Malhame R, Caines P (2019) A quantilized mean field game approach to energy pricing with application to fleets of plug-in electric vehicles. *Communication présentée à 58th IEEE Conference on Decision and Control (CDC 2019)* 299–304.

Wang Z, Yue D, Liu J, Xu Z (2019) A stackelberg game modelling approach for aggregator pricing and electric vehicle charging. *2019 IEEE 28th International Symposium on Industrial Electronics (ISIE)*, 2209–2213, URL `http://dx.doi.org/10.1109/ISIE.2019.8781294`.

Zeng B, Dong H, Sioshansi R, Xu F, Zeng M (2020) Bilevel robust optimization of electric vehicle charging stations with distributed energy resources. *IEEE Transactions on Industry Applications* 56(5):5836–5847, URL `http://dx.doi.org/10.1109/TIA.2020.2984741`.

Zhu Z, Lambotharan S, Chin WH, Fan Z (2016) A mean field game theoretic approach to electric vehicles charging. *IEEE Access* 4:3501–3510, ISSN 2169-3536, URL `http://dx.doi.org/10.1109/ACCESS.2016.2581989`.

Zou J, Ahmed S, Sun XA (2018) Partially adaptive stochastic optimization for electric power generation expansion planning. *INFORMS Journal on Computing* 30(2):388–401.

Zugno M, Morales JM, Pinson P, Madsen H (2013) A bilevel model for electricity retailers' participation in a demand response market environment. *Energy Economics* 36:182–197, ISSN 0140-9883, URL `http://dx.doi.org/https://doi.org/10.1016/j.eneco.2012.12.010`.

Appendices

A Formulation of the ETEM energy model

In this appendix, we present the formulation of the deterministic ETEM energy model. We mostly use a similar notation as in Aliakbarisani et al. (2020). However, we slightly depart from Aliakbarisani et al. (2020) where we use a regional demand response variable $\boldsymbol{V}$. Let us start with the definition of the sets. Set $\mathbb{T}$ indicates time periods, and $\mathbb{S}$ is the set of time slices inside a period. Set $\mathbb{C}$ is for energy commodities, and $\mathbb{P}$ identifies technologies. Input-output energy flows are shown in set $\mathbb{F}$. Finally, set $\mathbb{L}$ identifies buses in different geographical zones. A full nomenclature is presented Table 3.

Table 3: Nomenclature used in ETEM formulation

$t \in \mathbb{T}$	Index for time period	$\beta_{t,s,p}$	Capacity factor
$s \in \mathbb{S}$	Index for time-slices	η_c	Network efficiency
$p \in \mathbb{P}$	Index for technologies	$\eta^t_{f,f'}$	Technology efficiency
$c \in \mathbb{C}$	Index for energy commodities	$\lambda_{t,s,l,l',c}$	Transmission cost
$c_s \in \mathbb{CS}$	Index for energy storage	$\lambda'_{t,s,c}$	Export cost
$f \in \mathbb{F}$	Index for energy flows	$\lambda_{t,s,c}$	Import cost
$l \in \mathbb{L}$	Index for buses (geographical zones)	$\nu_{t,s,c}$	Maximum deviation from
$j \in \mathbb{J}$	Index for seasons		nominal demand response
$i \in \mathbb{I}$	Index for period-seasons (t, j)	$\nu_{t,p}$	Variable cost
$\mathbb{P}^C_c \subseteq \mathbb{P}$	Set of technologies consuming c	$\Omega_{t,l,p}$	Available capacity of technology p
$\mathbb{P}^P_c \subseteq \mathbb{P}$	Set of technologies producing c	$\pi_{t,p}$	Fixed production cost
$\mathbb{P}^R \subseteq \mathbb{P}$	Set of intermittent technologies	ρ	Discount factor
$\mathbb{C}^I \subseteq \mathbb{C}$	Set of imported commodities	θ^c_p	Proportion of output c from technology
$\mathbb{C}^{\mathcal{D}} \subseteq \mathbb{C}$	Set of useful demands		p that can be used in peak period
$\mathbb{C}^{EX} \subseteq \mathbb{C}$	Set of exported commodities	l_p	Life duration of technology p
$\mathbb{C}^{TR} \subseteq \mathbb{C}$	Set of transmitted commodities	$\Theta_{t,l,d}$	Annual final demand
$\mathbb{C}_f \subseteq \mathbb{C}$	Set of commodities linked to flow f	$\upsilon_{t,s,c}$	Nominal demand response
$\mathbb{C}^{\mathcal{G}} \subseteq \mathbb{C}$	Set of commodities with margin reserve	$\varrho_{t,s,c}$	Required reserve for commodity $c \in \mathbb{C}^{\mathcal{G}}$
$\mathbb{S}^j \subseteq \mathbb{S}$	Set of time-slices s in season j	$\boldsymbol{C}_{t,l,p}$	Variable for new capacity addition
$\mathbb{S}^s \subseteq \mathbb{S}$	Set of successive time-slices of s	$\boldsymbol{C}^T_{t,l,p}$	Total installed capacity
$\mathbb{S}^{\mathcal{G}} \subseteq \mathbb{S}$	Set of time-slices in peak period	$\boldsymbol{P}_{t,s,l,p,c}$	Variable for activity of technology p
$\mathbb{FI}_p \subseteq \mathbb{F}$	Set of inputs to technology p	$\boldsymbol{I}_{t,s,l,c}$	Variable for import
$\mathbb{FO}_p \subseteq \mathbb{F}$	Set of outputs from technology p	$\boldsymbol{E}_{t,s,l,c}$	Variable for export
$\alpha_{t,p}$	Investment cost	$\boldsymbol{T}_{t,s,l,l',c}$	Variable for regional transmission
		$\boldsymbol{V}_{t,s,l,d}$	Variable for demand response

$$\min \sum_{t,l} \rho^t \cdot \left(\sum_p \alpha_{t,p} \boldsymbol{C}_{t,l,p} + \pi_{t,p} (\sum_{k=0}^{l_p - 1} \boldsymbol{C}_{t-k,l,p} + \Omega_{t,l,p}) + \sum_{s,c} \nu_{t,p} \boldsymbol{P}_{t,s,l,p,c} + \right.$$

$$\sum_{s,c}(\lambda_{t,s,c}\boldsymbol{I}_{t,s,l,c} - \lambda'_{t,s,c}\boldsymbol{E}_{t,s,l,c}) + \sum_{s,l',c}\lambda''_{t,s,l,l',c}\boldsymbol{T}_{t,s,l,l',c}\Bigg), \tag{32a}$$

s.t.

$$(\sum_{p\in\mathbb{P}_c^P}\boldsymbol{P}_{t,s,l,p,c} + \boldsymbol{I}_{t,s,l,c})\eta_c + \sum_{l'\neq l}(\eta_c\boldsymbol{T}_{t,s,l',l,c} - \boldsymbol{T}_{t,s,l,l',c}) \geq \sum_{p\in\mathbb{P}_c^C}\boldsymbol{P}_{t,s,l,p,c} + \boldsymbol{E}_{t,s,l,c}$$

$$\forall\, t,s,l,c \in \mathbb{C}/\mathbb{C}^{\mathcal{D}} \tag{32b}$$

$$\Big(\sum_{l,p\in\mathbb{P}^c}\theta_p^c\cdot\beta_{t,s,p}(\sum_{k=0}^{l_p-1}\boldsymbol{C}_{t-k,l,p} + \Omega_{t,l,p}) + \sum_{l,p\in\mathbb{P}_c^P/\mathbb{P}_c}\theta_p^c\cdot\boldsymbol{P}_{t,s,l,p,c} + \boldsymbol{I}_{t,s,l,c}\Big)\cdot\varrho_{t,s,c}$$

$$\geq \sum_{l,p\in\mathbb{P}_c^C}\boldsymbol{P}_{t,s,l,p,c} + \boldsymbol{E}_{t,s,l,c} \quad \forall t,s\in\mathbb{S}^{\mathcal{G}}, c\in\mathbb{C}^{\mathcal{G}} \tag{32c}$$

$$\eta_c\sum_{p\in\mathbb{P}^{Pc}}\boldsymbol{P}_{t,s,l,p,c} = \sum_{p\in\mathbb{P}^{Cc},s'\in\mathbb{S}^s}\boldsymbol{P}_{t,s',l,p,c} \quad \forall t,s,l,c\in\mathbb{CS} \tag{32d}$$

$$\sum_{p\in\mathbb{P}_c^P}\boldsymbol{P}_{t,s,l,p,c} \geq \Theta_{t,l,c}\boldsymbol{V}_{t,s,l,c} \qquad \forall t,s,l,c\in\mathbb{C}^{\mathcal{D}} \tag{32e}$$

$$\upsilon_{t,s,l,c}(1-\nu_{t,s,l,c}) \leq \boldsymbol{V}_{t,s,l,c} \leq \upsilon_{t,s,l,c}(1+\nu_{t,s,l,c}) \quad \forall t,s,l,c\in\mathbb{C}^{\mathcal{D}} \tag{32f}$$

$$\sum_{s\in\mathcal{S}_j}\boldsymbol{V}_{t,s,l,c} = \sum_{s\in\mathcal{S}_j}\upsilon_{t,s,l,c} \qquad \forall t,l,c\in\mathbb{C}^{\mathcal{D}}, j\in\mathbb{J} \tag{32g}$$

$$\sum_{c:p\in\mathbb{P}_c^P}\boldsymbol{P}_{t,s,l,p,c} \leq \beta_{t,s,p}\left(\sum_{k=0}^{l_p-1}\boldsymbol{C}_{t-k,l,p} + \Omega_{t,l,p}\right) \qquad \forall t,s,l,p\notin\mathbb{P}^R, \tag{32h}$$

$$\sum_{c\in\mathbb{C}_m^p}\boldsymbol{P}_{t,s,l,p,c} = \beta_{t,s,p}\left(\sum_{k=0}^{l_p-1}\boldsymbol{C}_{t-k,l,p} + \Omega_{t,l,p}\right) \qquad \forall t,s,l,p\in\mathbb{P}^R \tag{32i}$$

$$\sum_{c\in\mathbb{C}_{f'}}\boldsymbol{P}_{t,s,l,p,c} = \eta_{f,f'}^t\cdot\sum_{c\in\mathbb{C}_f}\boldsymbol{P}_{t,s,l,p,c} \quad \forall f\in\mathbb{FI}_p, f'\in\mathbb{FO}_p, t,s,l,p \tag{32j}$$

$$(\boldsymbol{P},\boldsymbol{I},\boldsymbol{E},\boldsymbol{T})\in\mathcal{Y}\ ,\ \boldsymbol{C}\in\mathcal{X}\ ,\ \boldsymbol{P}\geq 0,\boldsymbol{I}\geq 0,\boldsymbol{E}\geq 0,\boldsymbol{T}\geq 0,\boldsymbol{C}\geq 0,\boldsymbol{V}\geq 0\,. \tag{32k}$$

Equation (32a) is the objective function which minimizes a discounted sum of all costs of the system over all regions ($l\in\mathbb{L}$) and time periods ($t\in\mathbb{T}$). The total cost include investment, fixed and operational costs of technologies, import, export and transmission costs of energy commodities. Variables $\boldsymbol{C},\boldsymbol{P},\boldsymbol{I},\boldsymbol{E},\boldsymbol{T}$ are capacity installation, energy production, import, export and regional transmission of energy, respectively. Parameters $\alpha_{t,p}$, $\nu_{t,p}$, $\lambda_{t,s,c}$, $\lambda'_{t,s,c}$, $\lambda''_{t,s,l,l',c}$, and $\pi_{t,p}$ are unit costs of the associated variables.

A commodity balance constraint is presented in (32b). It assures that during each period t and time-slice s, the regional procurement of energy commodity c is more or equal to the overall consumption. Total regional procurement, the left-hand side of the constraint, includes i) total production of commodity c in region l by all technologies producing it ($\mathbb{P}_c^P$), ii) import of commodity c, and iii) net transmission of commodity c into region l. It is worth mentioning that while import and export refers to the transfer of energy from outside of the boundary of the energy system, energy transmission is the amount of energy which is produced in one region and transmitted to another region inside the energy system. Input energy c is multiplied by parameter η_c, which is the efficiency of the network with respect to commodity c, e.g., the efficiency of electricity transmission lines. On the right-hand

side, the overall consumption of commodity c is equal to internal consumption by technologies $\mathbb{P}_c^C$, added to the amount of commodity that is exported.

In addition to the energy balance constraint (32b), for commodities in set $\mathbb{C}^{\mathcal{G}}$ constraint (32c) provides a safety margin, during peak time-slices $s \in \mathbb{S}^{\mathcal{G}}$, to protect against random events not explicitly represented in the model. Parameter $\varrho_{t,s,c} \in [0,\ 1]$ represents the fraction of reserved capacity needed to ensure covering the peak load. The left-hand side of this constraint models the maximum amount of commodity $c \in \mathbb{C}^{\mathcal{G}}$ that can be procured in period t and time-slice s. This amount is equal to the sum of i) the maximum production capacity of commodity c by technologies that produce it as their main output ($\mathbb{P}_c$), ii) the production of commodity c by technologies that produce c as their by-product of their main activity, and iii) the import of commodity c. The left-hand side is the total consumption similar to constraint (32b). Parameter θ_p^c is the proportion of technology production that can be used during the peak period. Constraint (32d) is a balance constraint for storage commodities. Namely, depending on the efficiency of the storage technology i.e., η_c, a fixed portion of the amount of storage at time-slice s can be restored at subsequent time-slice s'. Constraints (32e) - (32g) together are modeling the notion of demand response. Specifically, constraint (32e) ensures that for each commodity c in the set of useful demand $\mathbb{C}^{\mathcal{D}}$, the total production accounted for by variable $\boldsymbol{P}$ must satisfy the demand in each time slice and region. Parameter $\Theta_{t,l,c}$ is the total demand and variable $\boldsymbol{V}_{t,s,l,c}$ attempts to optimally distribute the total demand of period t into all time-slices $s \in \mathbb{S}$ inside period t and region l. Constraint (32f) limits the demand response to vary within a certain margin $\nu_{t,s,l,c}$ from the nominal value, i.e., $\upsilon_{t,s,l,c}$. In addition, since the shift of the demand is only possible between time slices in a day, constraint (32g) limits the sum of the demand response to be equal to the sum of the nominal values in each season.

Constraint (32h), known as capacity factor constraint, limits the maximum activity of each technology to the available capacity of that technology. Parameter $\beta_{t,s,p}$ is the capacity factor and simply represents the fraction of the total capacity which is available at each time-slice. In addition, constraint (32i) enforces that the production by renewable technologies take their maximum possible value considering the total available capacity of these technologies. Constraint (32j) defines the efficiency of technology p. Parameter $\eta_{f,f'}^t$ is the efficiency of technology p with output flow $f^{'} \in \mathbb{FO}_p$ and input flow $f \in \mathbb{FI}_p$.

Finally, space $\mathcal{X}$ and $\mathcal{Y}$ represent operational, technical, and economical constraints that define the structure of the energy network and a desirable space for capacity and procurement decisions. For example, constraints on CO_2 emissions, technology market penetration, technology ramping, total energy import and export are among the constraints that form up the space $\mathcal{X}$ and $\mathcal{Y}$. Since these constraints do not affect our analysis in this paper, we omit to report them and refer the reader to Babonneau et al. (2017) for a complete list of constraints.

B Differences between R-ETEM and Babonneau et al. (2020)

In Babonneau et al. (2020), the authors propose to robustify the deterministic version of ETEM presented in (1) by replacing constraint (3) with the robust constraint:

$$\Delta_{l,c}^{\min} \leq \sum_{t \in \mathbb{T}} \sum_{s \in \mathbb{S}} \Theta_{t,l,c} \boldsymbol{V}_{t,s,l,c} \leq \Delta_{l,c}^{\max},\ \forall\, l \in \mathbb{L}, c \in \mathbb{C}^{\mathcal{D}} \tag{33}$$

with

$$\Delta_{l,c}^{\min} := \sup_{\xi \in \hat{\Xi}} \sum_{(t,s) \in \mathbb{T} \times \mathbb{S}} \Delta_t^{l,c,-} + (\bar{\Delta}_t^{l,c} - \Delta_t^{l,c,-}) \xi_t$$

and

$$\Delta_{l,c}^{\max} := \inf_{\xi \in \hat{\Xi}} \sum_{(t,s) \in \mathbb{T} \times \mathbb{S}} \Delta_t^{l,c,+} + (\bar{\Delta}_t^{l,c} - \Delta_t^{l,c,+}) \xi_t$$

where $\hat{\Xi}$ is a budgeted uncertainty set in the non-negative orthant, while $[\Delta_t^{l,c,-}, \Delta_t^{l,c,+}]$ is a confidence region for the demand response at time t, and $\bar{\Delta}_t^{l,c}$ is the average value. We first note that (33) is a relaxation (therefore an optimistic approximation) of:

$$\Delta_t^{l,c,-} + (\bar{\Delta}_t^{l,c} - \Delta_t^{l,c,-}) \xi_t \leq \Theta_{t,l,c} \boldsymbol{V}_{t,s,l,c} \,, \; \forall \, \xi \in \hat{\Xi}, \, \forall \, (s,t,l,c) \in \mathbb{S} \times \mathbb{T} \times \mathbb{L} \times \mathbb{C}^{\mathcal{D}} \tag{34a}$$

$$\Theta_{t,l,c} \boldsymbol{V}_{t,s,l,c} \leq \Delta_t^{l,c,+} + (\bar{\Delta}_t^{l,c} - \Delta_t^{l,c,+}) \xi_t \,, \; \forall \, \xi \in \hat{\Xi}, \, \forall \, (s,t,l,c) \in \mathbb{S} \times \mathbb{T} \times \mathbb{L} \times \mathbb{C}^{\mathcal{D}} \,, \tag{34b}$$

which imposes a robust set of upper and lower bonds on the demand response plan in each time-slice. Thus, we can interpret any feasible solution of constraint (34) (and approximately (33)) as identifying a demand response that has a robust potential of being plausible with respect to the distribution that generated the statistics captured in $(\Delta_t^{l,c,-}, \bar{\Delta}_t, \Delta_t^{l,c,+})$. In particular, the constraint offers no protection against the demand response deviations captured by $(\Delta_t^{l,c,-}, \bar{\Delta}_t, \Delta_t^{l,c,+})$. This is especially noticeable when considering that $\Delta_{l,c}^{\min}$ and $\Delta_{l,c}^{\max}$ are both non-increasing and non-decreasing with respect to $\Delta_t^{l,c,-}$ and $\Delta_t^{l,c,+}$ respectively. This implies that has the observed demand response becomes more uncertain, constraint (33) actually becomes less restrictive for $\Theta_{t,l,c}$.

C Numerical algorithm to obtain the average optimal state of charge and demand

To compute the representative EV user's average optimal state of charge and average demand, one needs to numerically solve FBODEs $(14-15)$ to obtain (η_τ, w_τ). Then, the solution, $(\Psi_\tau, \Pi_\tau)_{\tau \in [0,T]}$ is obtained by solving the FBODEs $(21-22)$. Finally, we the average optimal state of charge and average demand is calculated with the feedback formula (28) and (27). This procedure is done with a simple implementation of the Euler Scheme. Algorithm 2 presents the detail of this implementation.

Algorithm 2: Euler Scheme for numerical computation of the MFG equilibrium

Discretize [0,T], into points $\tau \in \mathcal{T}$, with uniform gap $d\tau$;
Set $\eta_T = \bar{q}$;
for $\tau \in \mathcal{T}$ **do**
  $\eta_{\tau - d\tau} \leftarrow \eta_\tau - \big(\frac{\eta_\tau^2}{\kappa} - q\big) d\tau$
end
Set $w_0 = \frac{s^2 \eta_0^2}{\kappa^2}$
for $\tau \in \mathcal{T}$ **do**
  $w_{\tau + d\tau} \leftarrow w_\tau + \big(\frac{\epsilon^2 \eta_\tau^2}{\kappa^2} - w_\tau \frac{2q}{\eta_\tau}\big) d\tau$
end
Set $\Psi_T = 0$
for $\tau \in \mathcal{T}$ **do**
  $\Psi_{\tau - d\tau} \leftarrow \Psi_\tau - \big(F_1(\tau)\Psi_\tau^2 + F_2(\tau)\Psi_\tau + B_1(\tau)\Psi_\tau + B_2(\tau)\big) d\tau$
end
Set $\Pi_T = -\bar{q} a_T$
for $\tau \in \mathcal{T}$ **do**
  $\Pi_{\tau - d\tau} \leftarrow \Pi_\tau - \big(F_1(\tau)\Psi_\tau \Pi_\tau - F_3(\tau)\Psi_\tau + B_1(\tau)\Pi_\tau + B_3(\tau)\big) d\tau$
end
Set $m_0 = a_0$
for $\tau \in \mathcal{T}$ **do**
  $m_{\tau + d\tau} \leftarrow m_\tau + \big(- \frac{\eta_\tau m_\tau + \Pi_\tau}{\kappa + \Psi_\tau + \lambda(\tau)} - v_\tau \big) d\tau$
end
for $\tau \in \mathcal{T}$ **do**
  $\Delta_\tau \leftarrow - \frac{\eta_\tau m_\tau + \Pi_\tau}{\kappa + \Psi_\tau + \lambda(\tau)}$
end